ELSEVIER

Coordination Chemistry Reviews
153 (1996) 25–56

COORDINATION CHEMISTRY REVIEWS

Mo(W,V)–Cu(Ag)–S(Se) cluster compounds

Hong-Wei Hou [a], Xin-Quan Xin [a,*], Shu Shi [b]

[a] *State Key Laboratory of Coordination Chemistry, Department of Chemistry, Nanjing University, Nanjing 210093, China*

[b] *Optical Crystal Laboratory, Department of Chemical Engineering, National University of Singapore, Kent Ridge 0511, Singapore*

Received May 1 1995

Contents

* Corresponding author.

SSDI 0010-8545(95)01224-9

Abstract

This review summarizes the preparation, skeletal structure, reactions, spectroscopic properties and non-linear optical properties of Mo(W,V)–Cu(Ag)–S(Se) cluster compounds; 190 such compounds belong to 23 structural types; 25 reactions are classified into ligand substitution, addition and decomposition reactions. Recently, some Mo(W)–Cu(Ag)–S clusters were found to exhibit strong non-linear optical properties; the optical limiting threshold measured for $[(PPh_3)_4Ag_4Mo_2S_8]$ is one order of magnitude lower than that of C_{60}.

Keywords: Mo(W,V)–Cu(Ag)–S(Se) cluster compounds; Preparation; Skeletal structure; Reactions; Spectroscopic properties; Non-linear optical properties

1. Introduction

Cluster chemistry is one of the most important and active areas in inorganic and physical chemistry [1–4], because of the special roles played by clusters in catalysis reactions [5,6], biological processes [7] and advanced materials [8,9]. Historically, "electron-rich" clusters containing carbonyl, cyclopentadienyl, etc. were studied extensively [10,11]. Since the 1980s, the "electron-poor" clusters have also received much attention [12–14]; clusters containing Mo, Fe and S are among the most widely studied (as models for dinitrogenase).

The biological functions of Cu–Mo–S clusters were first recognized in ruminants [15]. Systematic investigations on "electron-poor" Mo(W,V)–Cu(Ag)–S(Se) clusters have yielded over 190 such compounds. They belong to 23 structural types. Some have already been reviewed [16–20]. Recently, certain Mo(W)–Cu(Ag)–S clusters were found to exhibit a strong non-linear optical (NLO) effect [21–30]. In a number of aspects they are comparable with or even better than the best NLO materials ever reported [31]. In this article, we bring the literature review in this field up to date.

2. Synthesis of Mo(W,V)–Cu(Ag)–S(Se) clusters

2.1. Synthesis via reactions in solution

Before the 1990s, nearly all the Mo(W,V)–Cu(Ag)–S(Se) clusters were synthesized via traditional solution reactions. The reaction usually involves thiometallates $MO_{4-n}S_n^{2-}$ ($M \equiv$ Mo, W, V; $n = 2, 3, 4$), M′L ($M' \equiv$ Cu, Ag; $L \equiv$ Cl, Br, I, CN, SCN, etc.) and sometimes organic ligands. With this traditional method, about 100 clusters with 15 different types of framework have been obtained [32]. Recently, it has been recognized that research along this route has progressed to such an extent that it is now increasingly difficult to synthesize new "electron-poor" clusters with novel structures using these typical starting materials, unless new synthetic pathways can be discovered. A useful synthetic variation is to replace Group VB or VIB thiometallates with Mo(W,V)–S clusters of low nuclearity, and to use S-containing organic

ligands or Cu(Ag) complexes. With this method, over 20 clusters with five types of skeleton have been discovered [32]. It has also been demonstrated that this method can be extended to incorporate Sn, Cr, Hg, Pb, Zn, Ni, Co, etc. into clusters [33–36].

2.2. Synthesis via reactions in the solid state

Recently, a method to synthesize Mo(W,V)–Cu(Ag)–S(Se) clusters by solid state reactions at low heating temperatures (less than 100 °C) [37,38] has been explored and has attracted some attention [39,40]. About 150 new Mo(W,V)–Cu(Ag)–S cluster compounds have been synthesized employing this method, 45 of which have been determined structurally. The clusters with new skeletal structures include a 20-nuclear supra-cage cluster $[Mo_8Cu_{12}S_{32}]^{4-}$ [41], twin nest-shaped clusters $[Mo_2Cu_6O_2S_6L_2I_4]^{4-}$ (L≡Br, I) [23,42] and "half-open" cubane-like clusters $[MOS_3(CuL)_3(\mu_2\text{-}L)]^{3-}$ (M≡Mo, W; L≡Br, I) [24,25,42].

3. Classification

We classify the existing Mo(W,V)–Cu(Ag)–S(Se) clusters into three categories: mono-Mo(W,V), di-Mo(W,V) and poly-Mo(W,V) clusters.

3.1. Mono-Mo(W,V) clusters

In Mo(W,V)–Cu(Ag)–S(Se) clusters, it is convenient to consider $MO_{4-n}X_n^{2-}$ (M≡Mo, W, V; X≡S, Se; n=2, 3, 4) moieties as coordination centres which bind to M′ or M′L species (M′≡Cu, Ag) through X bridges. MX_4^{2-} has a tetrahedral geometry with six X–X edges. Since each edge can bind one M′ or M′L (L is a ligand) unit, an MX_4^{2-} moiety can form dinuclear, trinuclear, tetranuclear, pentanuclear, hexanuclear and heptanuclear clusters with M′ or M′L units in a stepwise manner. In such a heptanuclear cluster, all of the six X–X edges have been coordinated. No more metal atoms can be accepted by direct bonding to the MX_4 centre. Six is hence the ultimate M′ uptake capacity of an MX_4^{2-} moiety.

3.1.1. Dinuclear clusters (one Mo(W) atom and one Cu(Ag) atom)

$MO_{4-n}S_n^{2-}$ (M≡Mo, W; n=2, 3, 4) binds one M′L (M′≡Cu, Ag) through two sulphur atoms to form a dinuclear structure with an $M'(S)_2M$ bridge (Fig. 1). The following clusters have been reported: $[(CNCu)MoS_4]^{2-}$ [43–45], $[Cu(SPh)MoS_4]^{2-}$ [46], $[(S\text{–}C_6H_4\text{–}p\text{-}Me)CuMoS_4]^{2-}$ [46], $[(CNAg)MS_4]^{2-}$ [45,47], $[(NCCu)MOS_3]^{2-}$ [45], $[(PhSCu)MoO_2S_2]^{2-}$ [48], $[(NCSCu)\text{-}MoS_4]^{2-}$ [19], $[(NH_2)_2CSCuMoO_2S_2]^{2-}$ [49], $[(o\text{-Phen})CuMS_4]^{2-}$ [19], $[(CNCu)MoOS_3]^{2-}\cdot 0.5H_2O$ [45], $[NH_4CuMS_4]$ [50,51], $[AgMS_4\cdot\gamma\text{-MePyH}]_n$ [52] and $[AgMoS_4\cdot\alpha\text{-MePyH}]_n$ [52] (M≡Mo, W). The last two compounds have an infinite chain structure.

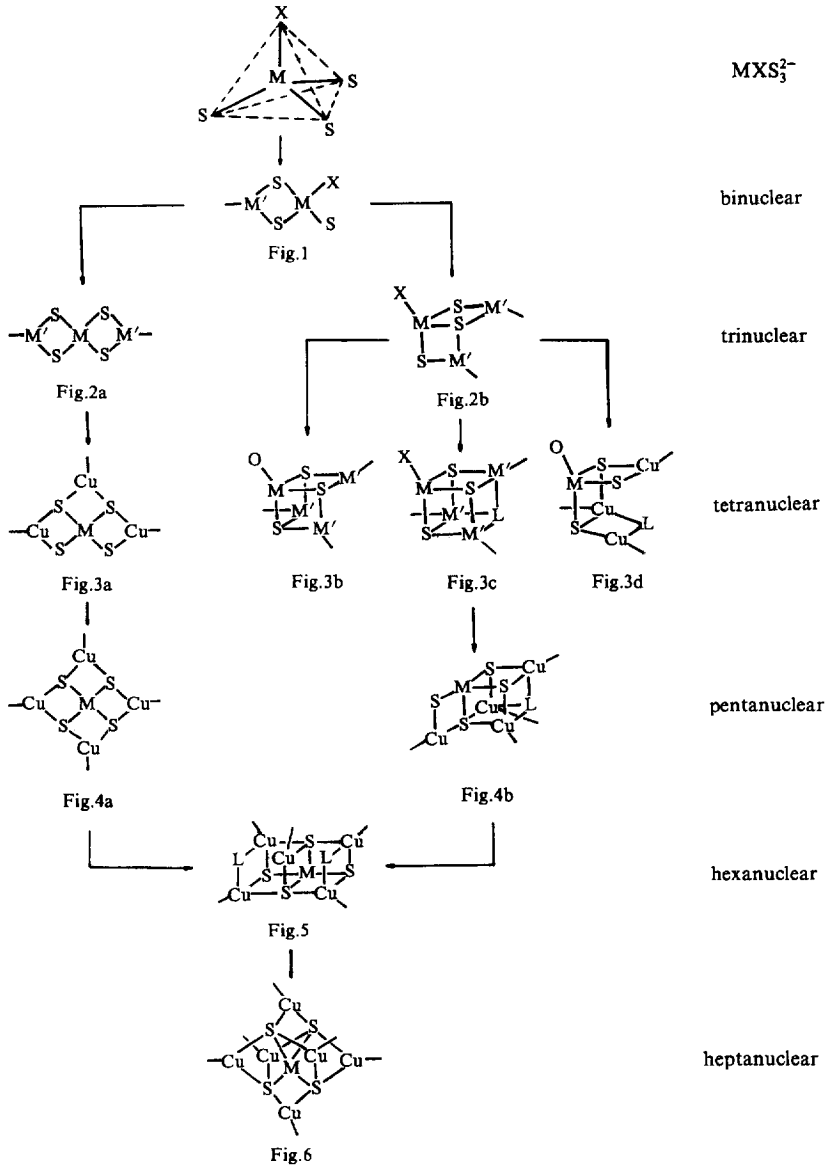

Scheme 1. The formation of mono-Mo(W,V) clusters.

3.1.2. Trinuclear clusters (one Mo(W) atom and two Cu(Ag) atoms)

These clusters belong to two structural types. The first contains MS_4^{2-} (M ≡ Mo, W) which acts as a tetradentate ligand bonding to two M′ (M′ ≡ Cu, Ag) atoms in a linear fashion (Fig. 2(a)). Clusters belonging to this group include $[(o\text{-Phen})_2Cu_2MS_4]$ [19], $[(CuCl)_2WS_4]^{2-}$ [53], $[(CuSPh)_2MoS_4]^{2-}$ [46],

$[(CuNCS)_2WS_4]^{2-}$ [54], $[(PhSC_2)_2Cu_2MoS_4]^{2-}$ [55], $[(CuBr)_2MoS_4]^{2-}$ [20], $[(CuCN)_2MoS_4]^{2-}$ [43,44], $[(CuCN)_2MS_4]^{2-}\cdot H_2O$ [45], $[(PMe_2Ph)_4Cu_2WSe_4]$ [56], $[(Py_2Cu)_2MoS_4]$ [57,58], $[(PPh_3)_4Cu_2WS_4]\cdot Py$ [59], $[(PMe_2Ph)_4Ag_2WSe_4]$ [56], $[(AsPh_3)_3Cu_2MS_4]$ [19], $[(PPh_3)_3Ag_2MS_4]\cdot 0.8CH_2Cl_2$ [18], $[(PPh_3)_3Ag_2MS_4]$ [60], $[(PPh_3)_3Ag_2WSe_4]$ [61], $[(PPh_3)_3Cu_2MS_4]\cdot 0.8CH_2Cl_2$ [62], $[(PPh_3)_3Ag_2WSe_4]\cdot 0.8CH_2Cl_2$ [47] and $[(PPh_3)_2Cu(AgCN)MoS_4]$ [63] (M≡Mo, W).

The second type contains two M′ (M′≡Cu, Ag) atoms bound to MOS_3^{2-} (M≡Mo, W) across two adjacent S–S edges with an angle M′–M–M′=90° (Fig. 2(b)). All of these clusters contain one terminal oxygen atom attached to M: $[(PPh_3)_3Cu_2MOS_3]$ [64], $[(PPh_3)_3Cu_2MOS_3]\cdot 0.8CH_2Cl_2$ [47], $[(PPh_3)_3Ag_2MOS_3]$ [65], $[Et_4N][(PPh_3)_3Ag(CuCN)WOS_3]$ [63], $[(PhSCu)_2MOS_3]^{2-}$ [43], $[(CuNCS)_2MOS_3]^{2-}$ [66] and $[(PPh_3)_2(Py)_2Cu_2MoOS_3]$ [67].

3.1.3. Tetranuclear clusters (one Mo(W,V) atom and three Cu(Ag) atoms)

Four structural types have been identified. The first structural type has three S–S edges of MS_4^{2-} (M≡Mo, W, V) tetrahedrally bound to three M′ (M′≡Cu, Ag) atoms with the angle M′–M–M′=90°. Two of the four S atoms are thrice bonded, the other two twice (Fig. 3(a)). Clusters belonging to this category include $[(CuCl)_3WS_4]^{2-}$ [68], $[(CuBr)_3MS_4]^{2-}$ [48] and $[(CuI)_3MS_4]^{2-}$ [48] (M≡Mo, W), where M′ is tri-coordinated, and $[(PPh_3)_4Cu_3VS_4]\cdot 2CH_2Cl_2$ [69] and $[(PPh_3)_4Cu_3VS_4]$ [69], where two of the three M′ atoms are tri-coordinated while the third is tetra-coordinated.

The cluster $[NEt_4]_2[(CuNCS)_3WS_4]$ [70] has an infinite one-dimensional polymer structure. Two of the three M′ atoms are tetrahedrally coordinated. The M′ atoms are all found in a tetrahedral environment in clusters containing bidentate chelating ligands, such as dtc [20], $[(S_2CNEt_2)_3Cu_3MS_4]^{2-}$ [71], $[(S_2CNC_5H_{10})_3Cu_3MoS_4]^{2-}\cdot DMF$ [72] and $[(dtcC_5H_{10})_3Cu_3MS_4]^{2-}$ [73] (M≡Mo, W). The cluster $[(PPh_3)_3(CN)Cu_3MoS_4]$ [74] has a mixed ligand set.

The second structural type of the tetranuclear clusters is a distorted cube with one missing corner (Fig. 3(b)). Three M′ atoms add on to the thiometallate. The MOS_3^{2-} unit therefore acts as a tridentate ligand. The O atom functions only as a terminal group. Clusters of this type include $[(CuCl)_3MOS_3]^{2-}$ [48], $[(S_2COEt)(PPh_3)_3Cu_3WOS_3]$ [75], $[BrCl_2Cu_3MoOS_3]^{2-}$ [26], $[(CuNCS)_3MOS_3]^{2-}$ [76] and $[\{S_2P(OEt)_2\}(PPh_3)_3Ag_3WOS_3]$ [77] (M≡Mo, W). Unlike the case of $[(CuNCS)_3WOS_3]^{2-}$, where polymerization occurs, only dimerization is observed in $[(CuNCS)_3MoOS_3]^{2-}$. Recently, we synthesized $[(Py)_5LCu_3MoOS_3]$ [78] (L≡Br, I) and $[(Py)_5ICu_3WOS_3]$ [42].

The third structural type has a cubane-like framework (Fig. 3(c)). Addition of a supplementary ligand L (L≡Cl, Br, I) to bridge the three Cu atoms produces this kind of structure. Clusters $[(PPh_3)_3Cu_3BrWS_4]$ [79], $[(PPh_3)_3Ag_3ClWS_4]\cdot 0.5P(S)Ph_3\cdot 3H_2O$ [80], $[(PPh_3)_3Cu_3IMoS_4]$ [79], $[(PPh_3)_3Ag_3BrWS_4]\cdot H_2O$ [81], $[(PPh_3)_3Ag_3IMoS_4]$ [80], $[Bu_4N]_3[I_3Ag_3BrMoS_4]$ [82], $[Bu_4N]_3[Cl_3Ag_3ClWS_4]$ [83,84], $[Bu_4N]_3[Br_3Ag_3BrMoOS_3]$ [83,84], $[Bu_4N]_3[Br_3Ag_3BrMoS_4]$ [83,85], $[Bu_4N]_3[Br_3Ag_3BrWS_4]$ [83,85], $[Bu_4N]_3[Br_3Cu_3BrWS_4]$ [86],

$[(AsPh_3)_3Cu_3BrWOS_3]$ [42], $[(AsPh_3)_3Cu_3IWOS_3]$ [42], $[(AsPh_3)_3Cu_3IMoS_4]$ [87] and $[(AsPh_3)_3Ag_3IWS_4](SAsPh_3)$ [42] belong to this category. They were synthesized by solid state reactions at low heating temperatures. The following clusters were synthesized in solution and belong to the same category: $[Cl_3Cu_3ClMS_4]^{3-}$ [20], $[(PPh_3)_3Cu_3ClWSe_4]$ [56], $[(PPh_3)_3Cu_3ClMS_4]$ [88], $[(PPh_3)_3Ag_3ClMS_4]$ [89], $[(PPh_3)_3Cu_3BrMS_4]$ [90,91], $[(PPh_3)_3Ag_3ClMOS_3]$ [92], $[(PPh_3)_3Cu_3BrMoOS_3]\cdot 0.5CH_2Cl_2$ [93], $[(AsPh_3)_3Cu_3ClMOS_3]$ [19], $[(AsPh_3)_3Cu_3ClMS_4]$ [19], $[(PPh_3)_3Cu_3BrMOS_3]$ [90], $[(PPh_3)_3Cu_3BrMoOS_3]\cdot 2THF$ [94] and $[(SCH_2CH_2S)(PPh_3)_3Cu_3BrMoOS_3]\cdot MeCN$ [95] (M≡Mo, W).

Recently, we synthesized several clusters having a "half- open" cubane-like skeleton (Fig. 3(d)) whose structure is between those shown in Figs. 3(b) and 3(c). These compounds include $[Et_4N]_3[(CuBr)_3(\mu_2\text{-Br})MOS_3]$ [24,25] (M≡Mo, W) and $[Et_4N]_3[(CuI)_3(\mu_2\text{-I})WOS_3]$ [42]. Their skeletons are composed of one M, three Cu, three μ_3-S and one μ_2-Br(or I) atoms. The M atom has basically retained the tetrahedral geometry of free $[MOS_3]^{2-}$. Three CuL (L≡Br, I) groups are bonded to the MOS_3 tetrahedron across three S–S edges. The fourth L atom bonds only with two of the three Cu atoms.

3.1.4. Pentanuclear clusters (one Mo(W,V) atom and four Cu(Ag) atoms)

Two types of structural arrangement are formed according to the relative positions of the four M′ atoms bonded to MS_4^{2-}. The first type has an "open" structure with five metal atoms in the same plane (Fig. 4(a)). Examples include dimeric $[(CuCl)_4WS_4]^{2-}$ [96,97], one- dimensional polymeric $[(CuBr)_4MoS_4]^{2-}$ [98], two-dimensional polymeric $[(CuSCN)_4MoS_4]^{2-}$ [99] and three-dimensional polymeric $[(CuSCN)_4WS_4]^{2-}$ [70]. The cluster $[(SCN)_5Cu_4WS_4]^{3-}$ [70] polymerizes in the form of linear chains of large 12-membered rings. Also belonging to this category are the clusters $[Py_4(SCN)_2Cu_4MS_4]$ [19], $[(\gamma\text{-pic})_4(SCN)_2Cu_4MS_4]$ [19] (M≡Mo, W), $[(CuBr)_4WS_4]^{2-}$ [98], $[(CuCl)_4MoS_4]^{2-}$ [97], $[(OC_4H_8dtc)(PhS)_3Cu_4VS_4]^{3-}$ [100], $[(OC_4H_8dtc)_2(PhS)_2Cu_4VS_4]^{3-}$ [100], $[(PhS)_4Cu_4VS_4]^{3-}$ [100], $[(Et_2dtc)_2(PhS)_2Cu_4VS_4]^{3-}$ [101] and $[(Et_2dtc)(PhS)_3Cu_4VS_4]^{3-}$ [101]. Clusters $[L_2Y_6Cu_4MS_4]$ [59] (M≡Mo, W; L≡Cl, Br, I; Y≡Py, γ-MePy), $[(\gamma\text{-MePy})_4Cu_4WS_4][W_6O_{19}]$ [102] and $[I_6Cu_4MS_4]^{4-}$ [103] (M≡Mo, W) were prepared by solid state reaction at low heating temperatures.

The second type has a cubane geometry with an additional face (Fig. 4(b)). Clusters $[(CuCl)_4ClMoS_4]^{3-}$ [20] and $[(CuCl)_4ClWS_4]^{3-}$ [20] are the only two reported clusters of this kind.

3.1.5. Hexanuclear clusters (one Mo(W) atom and five Cu atoms)

$[Cl_7Cu_5MS_4]^{4-}$ [104,105] (M≡Mo, W), $[Br_7Cu_5WS_4]^{4-}$ [106] and $[(CuPPh_3)_5Br_2VS_4]\cdot 0.5CH_2Cl_2$ [107] are the only structurally characterized clusters showing the double cubane-like structure (Fig. 5).

3.1.6. Heptanuclear clusters (one Mo(W,V) atom and six Cu atoms)

There are several such clusters reported. Their structures may be regarded as octahedral, in which MS_4 is surrounded by six Cu atoms (Fig. 6). They

include $[Cl_9Cu_6MoS_4]^{5-}$ [108], $[(CuPPh_3)_5(CuCl)Cl_2VS_4]\cdot CH_2Cl_2$ [109], $[(Py)_4I_4Cu_6MS_4]$ [106,110] and $[(Py)_4Br_4Cu_6MS_4]$ [86,111] (M≡Mo, W).

3.2. Di-Mo(W,V) clusters

About 40 di-Mo(W) clusters have been reported; the oxidation state of Mo(W) may be +6, +5 or +4. Di-M(VI) clusters are composed of two mono-M(VI) moieties (M≡Mo, W).

3.2.1. Trinuclear clusters (two Mo(W) atoms and one Cu(Ag) atom)

The first structural mode for this group of clusters has a linear M–Cu(Ag)–M skeleton (M≡Mo, W) as shown in Fig. 7(a). Examples are $[Cu(MS_4)_2]^{3-}$ [112] and $[Ag(MS_4)_2]^{3-}$ [112] (M≡Mo, W).

The second structural mode has an incomplete cubane-like, i.e. nest-shaped, skeleton (Fig. 7(b)). Clusters of this type include $[Et_4N][(PPh_3)(S_2C_2H_4)_2AgMo_2S_4]\cdot CH_{\{2\}Cl2}$ [113] and $[Et_4N][(CuPPh_3)M_2S_4(S_2C_2H_4)_2]$ [114] (M≡Mo, W). The oxidation state of Mo or W in these clusters is +4.

3.2.2. Tetranuclear clusters (two Mo(W,V) atoms and two Cu(Ag) atoms)

$[(PPh_3)_2Cu_2M_2S_4(SCH_2CH_2S)_2]$ [115,116] (M≡Mo, W), $[(PPh_3)_2Ag_2Mo_2S_4(TDT)_2]$ [117], $[(PPh_3)_2Cu_2Mo_2S_4(TDT)_2]EtOH\cdot H_2O$ [117], $[(PPh_3)_2CuAgMo_2S_4(TDT)_2]\cdot CH_2Cl_2$ [117], $[Cl_2Cu_2Mo_2S_4Cp_2]$ [118] and $[Et_4N]_4[(CuSCN)_2W_2S_4(SCN)_6]$ [119] have a cubane-like framework (Fig. 8). The oxidation state of Mo and W is +5. Only a few similar V–Cu–S [120] and V–Ag–S [121] clusters have been reported.

3.2.3. Pentanuclear clusters (two Mo(W) atoms and three Ag atoms)

Three clusters, $[Bu_4N]_2[(Et_2dtc)Ag_3M_2S_8]$ [122] (M≡Mo, W) and $[Bu_4N]_2[(C_6H_5CSS)Ag_3W_2S_8]$ [123], have been synthesized. Their structures are shown in Fig. 9. Five metal atoms are connected through two μ_3-bridging S atoms and four μ_2-bridging S atoms to form a five-membered ring. There are two terminal S atoms.

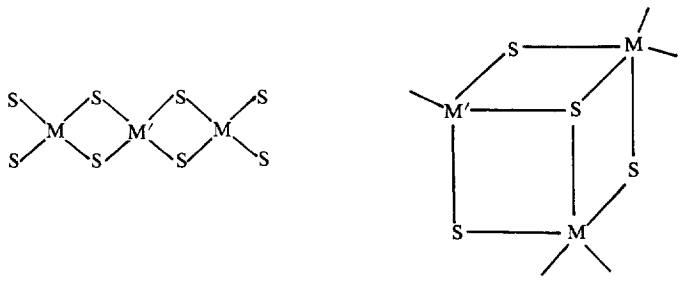

Fig. 7. Trinuclear clusters.

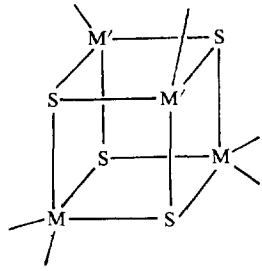

Fig. 8. Tetranuclear clusters.

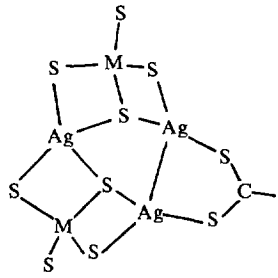

Fig. 9. Pentanuclear clusters.

3.2.4. Hexanuclear clusters (two Mo(W) atoms and four Cu(Ag) atoms)

In these clusters, e.g. $[(PPh_3)_4Ag_4M_2S_8]$ [124,125], $[(PPh_2Me)_4Ag_4M_2S_8]$ [60], $[(S_2CNC_4H_8)_2Cu_4M_2S_8]^{2-}$ [126], $[(PPh_3)_4Cu_4M_2S_6O_2]$ [127], $[(PPh_2Me)_4Cu_4M_2S_6O_2]$ [19], $[(AsPh_3)_4Ag_4W_2S_8]$ [128] and $[(P(C_7H_7)_3)_4Cu_4M_2S_6O_2]$ [129] (M≡Mo, W), the central unit is a new type of cage, formally yielding from the fusion of two six-membered metal–sulphur rings (Fig. 10). Here, the MXS_3^{2-} moiety acts as a quasi-quadruple bridge (bonds to all four M′ atoms) (X≡O, S; M′≡Cu, Ag).

3.2.5. Heptanuclear clusters (two Mo(W) atoms and five Cu atoms)

Two defective cubane-like, i.e. butterfly-shaped and nest- shaped, units $[MXS_3Cu_3]$ and $[MXS_3Cu_2]$ (X≡S, O; M≡Mo, W), linked through two S bridges, compose the framework (Fig. 11). The clusters of this category include

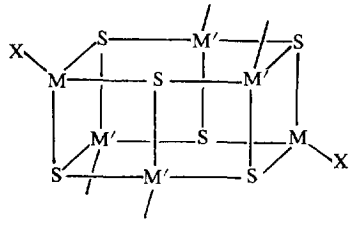

Fig. 10. Hexanuclear clusters.

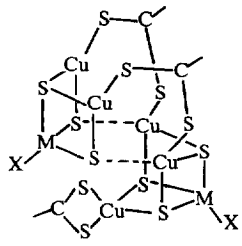

Fig. 11. Heptanuclear clusters.

$[(Et_2NCS_2)_3Cu_5M_2S_6O_2]^{2-}$ [130], $[(Me_2dtc)_3Cu_5M_2S_8]^{2-}$ [131], $[(Me_2dtc)_3Cu_5M_2S_6O_2]^{2-}$ [130] and $[(SCNEt_2)_3Cu_5M_2S_6O_2]^{2-}\cdot DMF$ [64] (M ≡ Mo, W).

3.2.6. Octanuclear clusters (two Mo(W) atoms and six Cu(Ag) atoms)

The cluster skeletons consist of two identical cubane-like fragments $[OMS_3Cu_3]$ (M ≡ Mo, W). The fragments are connected by two S-containing ligands acting as triple bridges (Fig. 12(a)). Examples include $[(PPh_3)_4(SCH_2CH_2OH)_2Cu_6Mo_2S_6O_2]$ [132], $[(PPh_3)_4(SCMe_3)_2Cu_6W_2S_6O_2]$ [75], $[(SCMe_3)_2(PPh_3)_4Ag_6W_2S_6O_2]$ [77] and $[(PPh_3)_4(SCMe_3)_2Ag_6Mo_2S_6O_2]$ [65].

Twin nest-shaped clusters $[Et_4N]_4[I_2L_2Cu_6I_2Mo_2S_6O_2]$ (L ≡ Br, I) [23,42] have also been prepared. The clusters contain two nest-shaped fragments interconnected through two I bridges (Fig. 12(b)).

3.3. Poly-Mo(W) clusters

Reports on poly-Mo(W) clusters are few. The oxidation state of Mo in icosanuclear clusters is six, whereas in other known poly-Mo(W) clusters it is lower.

3.3.1. Tri-Mo(W) clusters

The only structural type known has a cubane-like skeleton formed by one Cu atom and three Mo(W) atoms. Four metal atoms and four S atoms occupy eight corners of the cage (Fig. 13). $[CuMo_3S_4\{S_2P(OC_2H_5)_2\}_3(I)(\mu\text{-}CH_3COO)(Py)]$

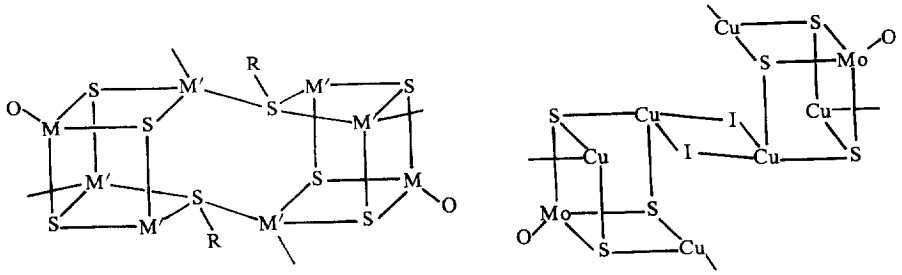

Fig. 12. Octanuclear clusters.

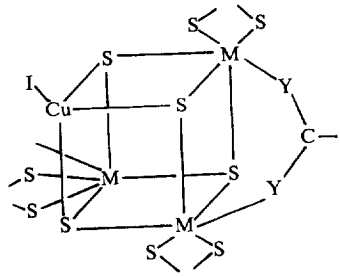

Fig. 13. Tri-Mo(W) clusters.

[133], $[CuMo_3S_4\{S_2P(OC_2H_5)_2\}_3(I)(\mu\text{-}CH_3COO)(DM\ F)]$ [134], $[CuMo_3S_4\{S_2P(OC_2H_5)_2\}_3(I)(\mu\text{-}CH_3COO)(CH_3CN)]$ [135], $[CuMo_3S_4\{S_2CN(OC_2H_5)_2\}_3(I)\{\mu\text{-}S_2CN_3(C_2H_5)_2\}(Py)]$ [136] and $[CuMo_3S_4\{S_2CN(OC_2H_5)_2\}_3(I)(O)_2(Py)]$ [136] are members of this family. The oxidation state of Mo or W in these clusters is +5.

3.3.2. Hexa-Mo clusters

Two kinds of hexa-Mo clusters have been reported. The first type, with six Mo atoms and two Cu atoms, forms a mixed-metal double cubane cluster $[\{(H_2O)_9Mo_3S_4CuCuS_4Mo_3(H_2O)_9\}(CH_3C_6H_5SO_3)_8]\cdot 12H_2O$ [137], as illustrated in Fig. 14(a). The oxidation state of Mo is 11/3, and the coordination number of Mo is six.

The second type of cluster, $[Et_4N]_2[(\mu_6\text{-}S)Cu_6S_6(S_2)_6Mo_6O_6](DMF)$ [138], is formed with six Mo atoms and six Cu atoms. The Cu atoms assume a distorted octahedral arrangement with a μ_6-S in the centre. This octahedron is compressed along the threefold axis due to the existence of weak Cu–Cu bonds (Fig. 14(b)). Six $(S_2)MoO$ moieties each coordinate with two Cu atoms through two S atoms. The valence of Mo is +5.

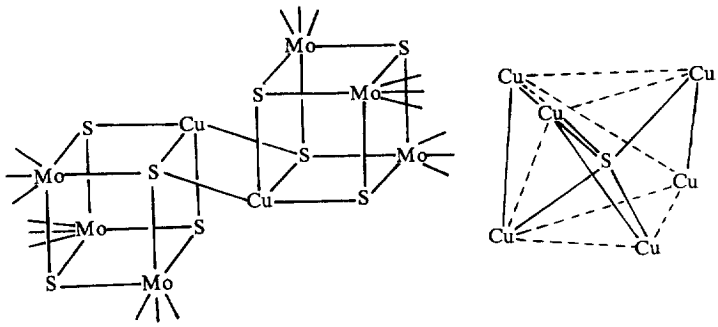

Fig. 14. Hexa-Mo clusters.

3.3.3. Octa-Mo(W) clusters

Cluster $[Bu_4N]_4[Cu_{12}Mo_8S_{32}]$ [41] (Fig. 15) is composed of eight nest-shaped Mo–3Cu units interconnected by shared Cu atoms. Its structure can also be formally described as a supra-cubic cage with eight Mo atoms at the corners and 12 Cu atoms each in the middle of the 12 edges. The metal atoms are coordinated through μ_2-, μ_3- and μ_4-bridging S atoms. Each metal atom (Mo or Cu) is surrounded by four sulphur atoms.

3.4. Summary of classification

In accordance with the classification given above, the following conclusions can be drawn.

(1) In all of the clusters, the oxidation state of all M′ atoms is +1 and oxygen atoms only act as terminal groups and do not bind to M′ (Cu, Ag) atoms.
(2) M (Mo, W, V) and M′ atoms are connected through two S bridging atoms in the form of an $M(S)_2M'$ four-atom ring.
(3) Eleven structural types of mono-Mo(W) clusters, from dinuclear to heptanuclear, have been reported.
(4) In all of the M(VI)–S–M′ (M ≡ Mo, W) clusters, di-Mo(W) and poly-Mo(W) clusters may be regarded as being composed by the fusion of several mono-Mo(W) clusters.
(5) The clusters containing low valence Mo or W are few, and the coordination number of Mo or W can be higher than four.

4. Reactions

Mo(W,V)–Cu(Ag)–S(Se) cluster compounds are composed of two parts: a cluster framework and outside ligands. The cluster skeleton is usually formed through different connection modes of the structural units, $M(S)_2M'$ (M ≡ Mo, W, V; M′ ≡ Cu, Ag). The reactions can be roughly classified into two types: ligand substitution

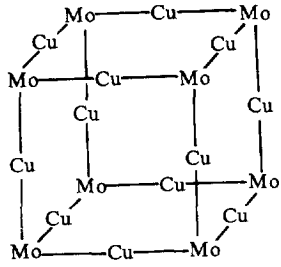

Fig. 15. Octa-Mo(W) clusters.

(where the cluster skeletons are untouched) and skeleton reactions (addition, decomposition).

4.1. Substitution reactions

Some terminal ligands, such as Cl^-, Br^- and I^-, are only loosely bound. They can be substituted by stronger ligands such as PPh_3 and Py to produce new compounds with identical skeletal structures. Examples of such reactions are shown in Scheme 2 (M ≡ Mo, W).

Terminal O atoms can be substituted by a ligand to produce a novel cluster. Only one such reaction has been reported (Scheme 3).

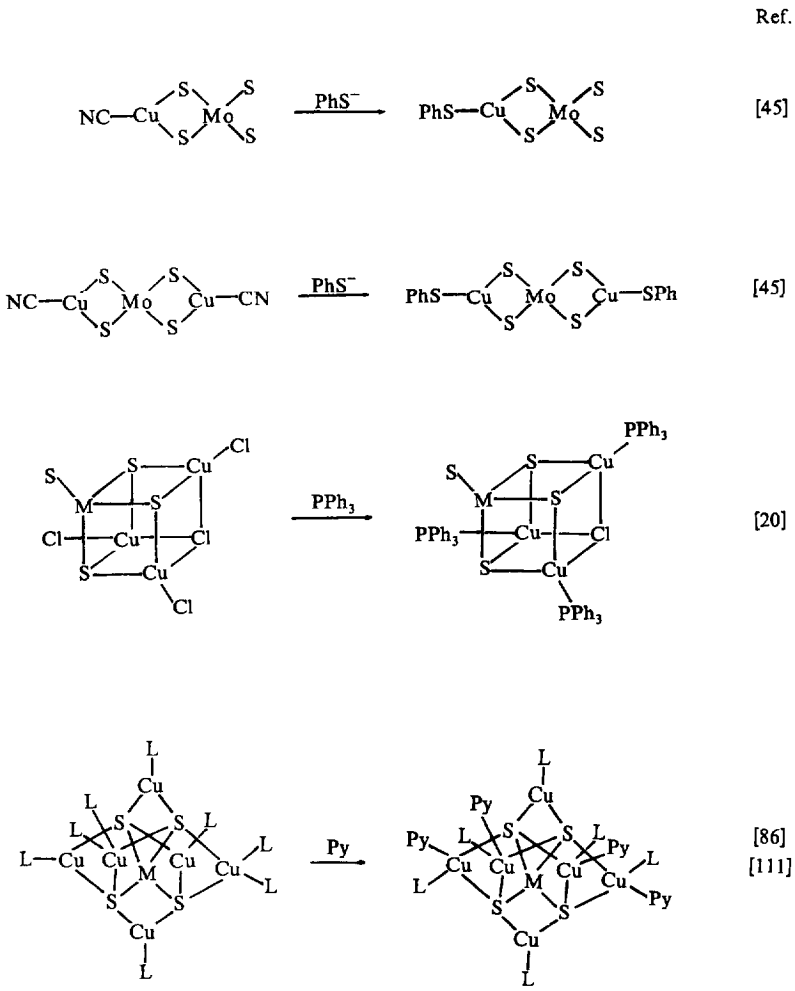

Scheme 2. Substitution reactions of ligands.

Ref.

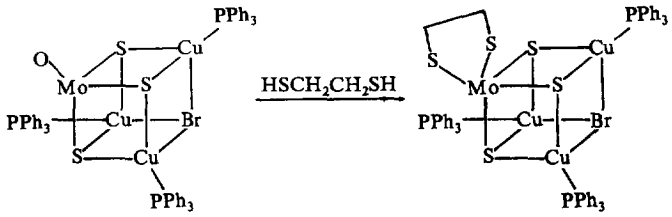

[95]

Scheme 3. Substitution reactions of terminal O atom.

4.2. Skeleton reactions

4.2.1. Addition reactions

One or several M'L moieties (M' ≡ Cu, Ag; L ≡ Cl, Br, I, etc.) can be added to a cluster of lower nuclearity to form a cluster of higher nuclearity. The prerequisite to bring about such a reaction is that the S atoms in the reactant cluster should be in an unsaturated coordination environment. For example, in a mono-Mo(W) heptanuclear cluster, each of four S atoms is coordinated tetrahedrally by four metal atoms and reaches coordination saturation. It can no longer accept an M'L moiety. Clusters containing sulphido ligands with unused lone pair electrons may coordinate to another metal complex which has coordinatively unsaturated metal sites or easily replaceable ligands. This is the basis of so-called "unit construction" [75].

Known reactions of this type are included in Schemes 4(a)–4(f) (M ≡ Mo, W). They include 2 (binuclear)+1 (mononuclear) reactions (Scheme 4(a)), 3 (trinuclear)+1 (mononuclear) reactions (Scheme 4(b)), 4 (tetranuclear)+1 (mononuclear) reactions (Scheme 4(c)), (3+1)+(3+1) reaction (Scheme 4(d)) and 3+3 reaction (Scheme 4(e).

Cluster "monomers" can dimerize or polymerize through unsaturated S atoms. "Co polymerization" of different "monomers" may lead to composite clusters. For instance, the 20-nuclear cluster $[W_8Cu_{12}O_4S_{28}]^{4-}$ can be formed by solid state reaction at low heating temperatures from a cubane-like unit and WOS_3^{2-} (Scheme 4(f)).

The largest Mo(W)–Cu(Ag)–S cluster, $[Mo_8Cu_{12}S_{32}]^{4-}$, has many unsaturated S atoms. Under appropriate conditions, it may probably be made to react with more M'L units to generate clusters of even higher nuclearity.

4.2.2. Decomposition reactions

Clusters of high nuclearity may decompose into clusters of lower nuclearity in the presence of excess ligand. The reaction usually starts as ligand substitution of an M'–S (M' ≡ Cu, Ag) unit. Examples are given in Scheme 5. Sometimes, this can be used effectively to lower deliberately the nuclearity of a cluster.

Ref.

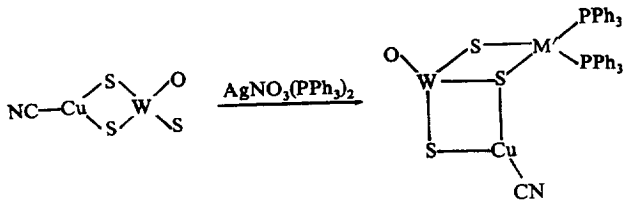

[63]

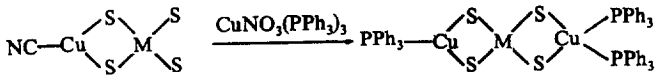

[45]

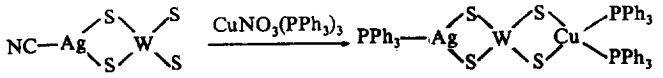

[45]

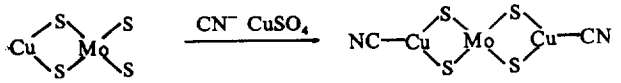

[45]

Scheme 4(a). 2+1 reactions.

Ref.

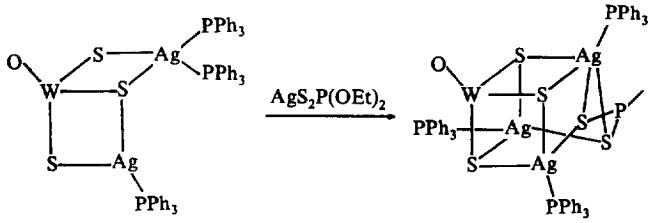

[77]

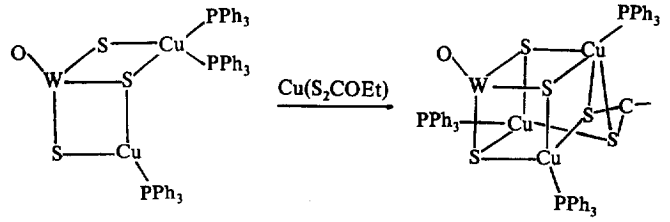

[75]

Scheme 4(b). 3+1 reactions.

Ref.

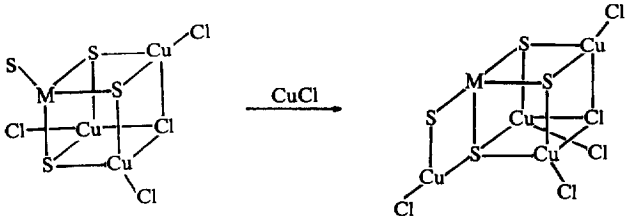

[20]

Scheme 4(c). 4+1 reactions.

Ref.

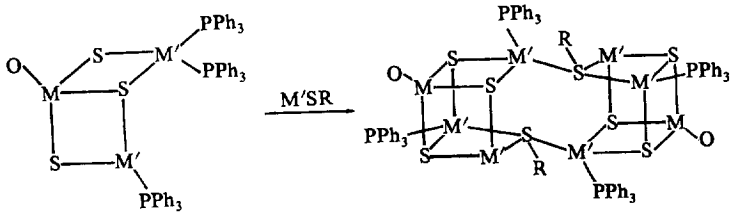

[65][75]
[77][132]

Scheme 4(d). (3+1)+(3+1) reactions.

Ref.

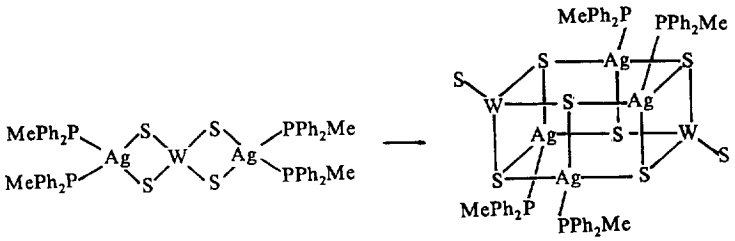

[60]

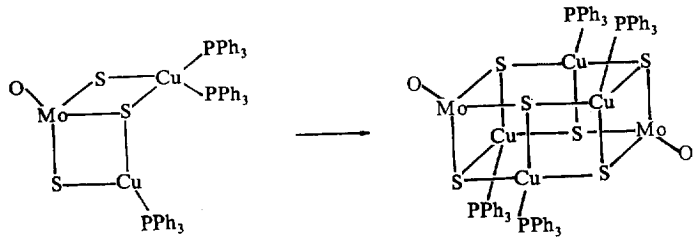

[47]

Scheme 4(e). 3+3 reactions.

Ref.

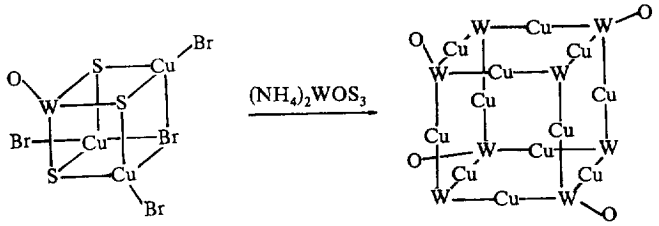

[42]

Scheme 4(f). "Co polymerization" reactions.

Ref.

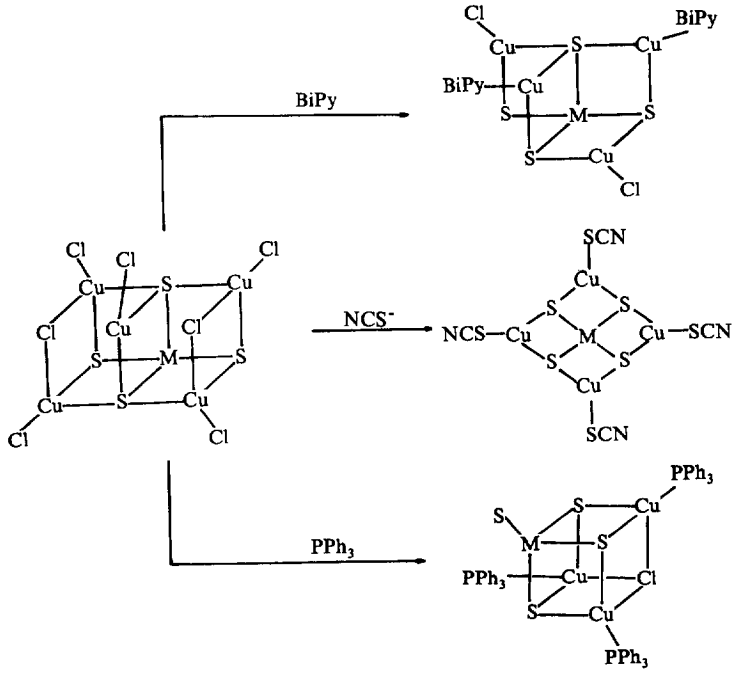

[104]

[104]

[104]

Scheme 5. Decomposition reaction.

In addition, redox reactions can often take place in these clusters. Thus the cyclic voltammogram of $[(n\text{-}Bu)_4N]_2[BrCl_2Cu_3MoOS_3]$ contains two quasi-reversible redox couples ($E_{pa1} = 0.40$ V and $E_{pc1} = 0.51$ V; $E_{pa2} = -1.75$ V and $E_{pc2} = -1.53$ V) [26]. The reaction may be visualized as $[BrCl_2Cu_3MOS_3]^{2-} \rightleftharpoons [BrCl_2Cu_3MOS_3]^{3-} \rightleftharpoons [BrCl_2Cu_3MOS_3]^{4-}$.

5. Spectra

5.1. UV–visible spectra

The assignment of the electronic transitions in simple oxo, thio and seleno anions of transition metals (Mo, W, V) with T_d and C_{3v} symmetry was studied 20 years ago [139–142]. Some of the general assignments are applicable to the Mo(W,V)–Cu(Ag)–S(Se) clusters synthesized later. There is a general consensus that the three strong absorptions (ν_1, ν_2, ν_3) are attributable to ligand-to-metal charge transfer transitions within the $MO_{4-n}S_n^{2-}$ unit. The band ν_1 near 467 nm in MoS_4^{2-}, 392 nm in WS_4^{2-}, 556 nm in $MoSe_4^{2-}$ and 463 nm in WSe_4^{2-} corresponds to a $1t_1 \rightarrow 2e$ transition, i.e. from the highest occupied molecular orbital (HOMO) to the lowest unoccupied molecular orbital (LUMO). The absorption of ν_2 is at 317 nm in MoS_4^{2-}, 277 nm in WS_4^{2-}, 310 nm in $MoSe_4^{2-}$ and 316 nm in WSe_4^{2-} and is attributed to a $t_1 \rightarrow 4t_2$ transition [143]. The absorption of ν_3 at 242 nm in MoS_4^{2-}, 216 nm in WS_4^{2-}, 269 nm in $MoSe_4^{2-}$ and 242 nm in WSe_4^{2-} is assigned to a $3t_2 \rightarrow 2e$ transition [143]. (Many assignments were supported by various MO calculations [144–147].)

The electronic spectra of Mo(W)–Cu(Ag)–S(Se) clusters are roughly comparable with the absorption bands of MXX'_3^{2-} (M ≡ Mo, W; X ≡ S, O; X′ ≡ S, Se). On the other hand, because the ligand-to-metal charge transfer bands are more or less affected by the coordination of Cu(Ag) to MXX'_3^{2-}, shifting of these electronic transition bands is observed. Table 1 gives the wavelengths of the electronic transitions of a few selected compounds.

In accordance with the data in Table 1, it can be seen that after coordination of the MXS_3^{2-} moieties to the M′L units, the ν_1 bands are shifted in the direction of longer wavelength in M–Cu–S clusters, and the higher the nuclearity, the longer the wavelength of the ν_1 band. The position of ν_1 can be observed in the region of shorter wavelength in M–Ag–S clusters. In M–Cu(Ag)–Se clusters, the maximum absorption peaks are always at longer wavelengths than ν_1 in the MSe_4^{2-} moiety.

5.2. IR spectra

For the free MX_4^{2-} (M ≡ Mo, W; X ≡ S, Se) ion, four vibrational modes are expected: $T_d = A_1(\nu_1) + E(\nu_2) + 2F_2(\nu_3, \nu_4)$. ν_1 and ν_2 are IR forbidden. In cluster compounds, the $[MX_4]$ moiety may have a lower symmetry. This leads to splitting of ν_2, ν_3 and ν_4, and makes ν_1 and ν_2 IR active [148]. $\nu_2(E)$ and $\nu_4(F_2)$ bands can be observed in the far-IR region, with $\nu_2 < \nu_4$ [148,149]. ν_3 and ν_1 are located in the region 400–500 cm^{-1}, with $\nu_3 > \nu_1$. The free MOX_3^{2-} ion has six vibrational modes $C_{3v} = 3A_1(\nu_1,\nu_3) + 3E(\nu_4,\nu_5,\nu_6)$ [141]. After coordination of the Cu(Ag) atoms with the MOX_3^{2-} moiety, these transitions are IR active and ν_4, ν_5 and ν_6 exhibit splitting. ν_3, ν_5 and ν_6 bands cannot be found in the IR region. ν_1 is in the range 800–1000 cm^{-1}, and ν_4 is located at about 450 cm^{-1}. The IR spectral parameters of various compounds are listed in Table 2.

It can be seen from Table 2 that the higher the nuclearity of the W–Cu–S cluster,

Table 1
Electronic absorption peaks (nm) of some Mo(W)–Cu(Ag)–S cluster compounds

Compounds	Electronic absorption					Reference
	ν_1	ν_2	ν_3	ν_4	ν_5	
MoS_4^{2-}	467	317	242			
$MoOS_3^{2-}$	465	392	323	260	227	
$[PPh_4][(o\text{-phen})CuMoS_4]$	495	338	260,242			[19]
$[PPh_4]_2[(CuNCS)MoS_4]$	495	338	258,242			[19]
$[PPh_4]_2[(CuCN)MoS_4]$	472	451,318	247,224			[19]
$[PPh_4]_2[(PhSCu)MoS_4]$	480	350,328	286,240			[19]
$[PPh_4]_2[(PhSCu)_2MoS_4]$	495	370,342	284,245			[19]
$[PPh_4]_2[(CuNCS)_2MoS_4]$	494	348	316			[70]
$[(o\text{-phen})_2Cu_2MoS_4]$	495	375	258,242			[19]
$[(PPh_3)_3Cu_2MoS_4]\cdot 0.8CH_2Cl_2$	490	370				[19]
$[Bu_4N]_2[BrCl_2Cu_3MoOS_3]$	500	408	286			[26]
$[(Py)_5BrCu_3MoOS_3]$	488	402	280,244			[78]
$[(Py)_5ICu_3MoOS_3]$	480	402	284,240			[78]
$[NEt_4]_3[(\mu_2\text{-Br})(CuBr)_3MoOS_3]$	516	366	296,270			[42]
$[NEt_4]_4[I_6Cu_4MoS_4]$	515	403	301,269			[103]
$[PPh_4]_2[(CuNCS)_4MoS_4]$	510	360				[70]
$[NEt_4]_2[(CuNCS)_4MoS_4]$	510	360				[70]
$[NEt_4]_3[Cu_4(NCS)_5MoS_4]$	504	360				[70]
$[(\gamma\text{-pic})_4(NCS)_2Cu_4MoS_4]$	490	370	245,210			[19]
$[Py_4(SCN)_2Cu_4MoS_4]$	490	370	245,210			[19]
$[NEt_4]_2[(CuCl)_5Cl_2MoS_4]$	512	360	308			[104]
$[(Py)_4Br_4Cu_6MoS_4]_n$	530	350	295			[111]
$[NEt_4]_4[Br_2I_4Cu_6Mo_2O_2S_6]$	500	410,310	288,240			[23]
$[NEt_4]_4[I_6Cu_6Mo_2O_2S_6]$	495	408	288			[42]
WS_4^{2-}	392	277	216			
WOS_3^{2-}	374	334	270	243		
$[^nPr_4N]_2[(CuCN)WS_4]$	396	284				[53]
$[(o\text{-phen})_2Cu_2WS_4]$	405	340	250,240			[19]
$[PPh_4]_2[(CuNCS)_2WS_4]$	416	310	292			[70]
$[^nPr_4N]_2[(CuCN)_2WS_4]$	409	398	291			[53]
$[PPh_4]_2[(CuCl)_2WS_4]$	424	296				[53]
$[PPh_4]_2[(CuCl)_3WS_4]$	432	350	308			[68]
$[NEt_4]_3[(\mu_2\text{-Br})(CuBr)_3WOS_3]$	445	330	310,262			[24]
$[(AsPh_3)_3IAg_3WS_4](SAsPh_3)$	355	310	236			[42]
$[(AsPh_3)_3BrCu_3WOS_3]$	425	260	236			[42]
$[(AsPh_3)_3ICu_3WOS_3]$	438	260	236			[42]
$[NEt_4]_2[(CuNCS)_3WS_4]$	422	308	290			[70]
$[biPy_2Cl_{1.75}Cu_{3.75}WS_4]$	432	328	270			[104]
$[PPh_4]_2[(CuNCS)_4WS_4]$	430	320				[70]
$[NEt_4]_3[Cu_4(NCS)_5WS_4]$	424	320	290			[70]
$[(\gamma\text{-pic})_4(NCS)_2Cu_4WS_4]$	405	335	224			[19]
$[Py_4(SCN)_2Cu_4WS_4]$	408	335	255,252			[19]
$[(AsPh_3)_4Ag_4W_2S_8]$	356	310	243			[128]
WSe_4^{2-}	463	316	242			
$[(PMePh_2)_4Cu_2WSe_4]$	485	323				[56]
$[(PMePh_2)_4Ag_2WSe_4]$	510	470	455			[56]
$[(PPh_3)_3ClCu_3WSe_4]$	490	338				[56]

the higher the frequencies of the W–O_t vibrations. Compared with the W–Cu–S compounds, the isostructural W–Ag–S compounds show higher W–O_t vibrational frequencies. Similarly, the W–O_t vibrational frequencies are always higher than the Mo–O_t frequencies when isostructural Mo–Cu(Ag)–S and W–Cu(Ag)–S clusters are compared.

5.3. NMR spectra

The solid state structures of Mo(W,V)–Cu(Ag)–S(Se) clusters can be established by single-crystal X-ray structure determination. Raman and IR spectroscopy can also be used to obtain information about the symmetry in solid samples [43,46]. However, it is more difficult to determine the structures of these clusters in solution, but NMR spectroscopy can be used in some cases. Table 3 summarizes some ^{95}Mo, ^{183}W, ^{33}S and ^{77}Se NMR spectra.

The data in Table 3 show that the Mo (or W) chemical shift decreases monotonically as the M′ to M ratio (M′ ≡ Cu, Ag; M ≡ Mo, W) increases [48]. Thus the Mo (or W) chemical shift of an Mo(W)–Cu(Ag)–S(Se) cluster provides an indirect measure of its skeletal structure. When a W cluster is compared with an Mo cluster with an identical structure, the W chemical shift is always about 1000 ppm larger than the Mo chemical shift. Compared with M–Cu–S clusters, the M chemical shift of M–Ag–S clusters is always larger. Smaller variations in the M chemical shift result from a change in the X ligand attached to the M′ atom (X ≡ Cl, Br, I, CN, PhS, etc.).

Table 3 also shows that the chemical shifts of ^{95}Mo and ^{183}W decrease when terminal S atoms are substituted by O atoms. A direct comparison of ^{95}Mo chemical shifts in $[(PhSCu)MoS_4]^{2-}$ and $[(PhSCu)MoO_2S_2]^{2-}$ shows that the difference is about 1300 ppm [48].

Only one ^{33}S NMR resonance signal is seen for all the binuclear and trinuclear clusters. The known facile M′L migration over different S sites leads to an exchange averaged signal for the thio ligand sites. Substitution of Ag for Cu in both the Mo and W compounds results in a decrease in the ^{33}S chemical shift [150].

Se chemical shifts increase as the nuclearity of the Mo(W)–Cu(Ag)–Se cluster increases. Two peaks are found in the ^{77}Se NMR spectrum of $[(PPh_3)_3Cu_3ClWSe_4]$; the resonance at 1232 ppm probably arises from the terminal Se nucleus [56].

5.4. Cyclic voltammetry

Compounds of the type $[M'(MO_{4-n}S_n)_2]^{2-}$ (M′ ≡ Fe, Co, Ni, Pb, etc.; M ≡ Mo, W; $n=2$, 3, 4) and $[(FeCl_2)_2MoS_4]^{2-}$ show reversible redox behaviour [152–154]. For example, $[Co(WS_4)_2]^{2-}$ at −0.49 V and −0.60 V and $[Fe(WS_4)_2]^{2-}$ at −0.15 V and −0.25 V [18]. Because of the complexity of the cyclic voltammograms of Mo(W)–Cu(Ag)–S clusters, only a few studies have been reported. Table 4 gives the cyclic voltammetry data of Mo(W)–Cu(Ag)–S clusters.

The cyclic voltammograms of these clusters are characterized by one quasi-reversible redox couple. Potentials observed at 0.41 V and 0.54 V in the

Table 2
IR absorption peaks (cm^{-1}) of some Mo(W)–Cu(Ag)–S cluster compounds (M≡Mo, W; X≡O, S, Se; X′≡S, Se)

Compound	$M–X_t$	$M–X'_{Br}$	Reference
$[PPh_4]_2[(CuNCS)MoS_4]$	485,495	440,450	[19]
$[PPh_4]_2[(CuCN)MoS_4]$	486,500	416,447	[19]
$[PPh_4]_2[(PhSCu)MoS_4]$	491	440,479	[19]
$[Et_4N][(CuCN)MoOS_3]$	893	499,462,424	[45]
$[Et_4N]_2[(CuCN)_2MoS_4]\cdot H_2O$		475,434	[45]
$[(PPh_3)_3Cu_2MoOS_3]$	910	492,465,440	[64]
$[(PPh_3)_3Ag_2MoS_4]\cdot 0.8CH_2Cl_2$		467,458	[88]
$[(PPh_3)_2(Py)_2Cu_2MoOS_3]$	903	467,451	[67]
$[PPh_4]_2[(PhSCu)_2MoS_4]$		462,470	[19]
$[PPh_4]_2[(CuNCS)_2MoS_4]$		467	[70]
$[(o\text{-phen})_2Cu_2MoS_4]$		460	[19]
$[(PPh_3)_3Cu_2MoS_4]\cdot 0.8CH_2Cl_2$		465	[19]
$[(PPh_3)_3Cu_3ClMoOS_3]$	908	451,444	[88]
$[(PPh_3)_3Cu_3ClMoS_4]$	515	447,441	[88]
$[(PPh_3)_3Cu_3IMoS_4]$	490	466	[79]
$[(AsPh_3)_3Cu_3IMoS_4]$	527	443	[42]
$[(PPh_3)_3Ag_3IMoS_4]$	516	433	[80]
$[Bu_4N]_2[(CuNCS)_3MoOS_3]$	881	436	[76]
$[Bu_4N]_3[Br_3Ag_3BrMoOS_3]$	907	438	[83]
$[Et_4N]_3[(\mu_2\text{-}I)(CuI)_3MoOS_3]$	911	442	[42]
$[Bu_4N]_2[BrCl_2Cu_3MoOS_3]$	920	444	[26]
$[(Py)_5BrCu_3MoOS_3]$	925	445	[78]
$[(Py)_5ICu_3MoOS_3]$	914	440	[78]
$[NEt_4]_3[(\mu_2\text{-}Br)(CuBr)_3MoOS_3]$	911	445	[25]
$[NEt_4]_4[I_6Cu_4MoS_4]$		442	[103]
$[PPh_4]_2[(CuNCS)_4MoS_4]$		445	[70]
$[PPh_4]_2[(CuNCS)_4MoS_4]$		458,447	[70]
$[NEt_4]_3[Cu_4(NCS)_5MoS_4]$		419	[70]
$[(\gamma\text{-pic})_4(NCS)_2Cu_4MoS_4]$		450	[19]
$[Py_4(SCN)_2Cu_4MoS_4]$		450	[19]
$[(PPh_3)_4Ag_4Mo_2S_8]$	515	453,438	[124]
$[NEt_4]_2[(CuCl)_5Cl_2MoS_4]$		460,448,428	[104]
$[(Py)_4Br_4Cu_6MoS_4]_n$		438	[111]
$[Et_4N]_2[(Me_2NCS_2)_3Cu_5Mo_2O_2S_6]$	900	450,438,415	[132]
$[NEt_4]_4[Br_2I_4Cu_6Mo_2O_2S_6]$	913	447	[23]
$[NEt_4]_4[I_6Cu_6Mo_2O_2S_6]$	901	447	[42]
$[^nPr_4N]_2[(CuCN)WS_4]$	490,482	450,444,415	[53]
$[(o\text{-phen})_2Cu_2WS_4]$		450	[19]
$[PPh_4]_2[(CuNCS)_2WS_4]$		455	[70]
$[^nPr_4N]_2[(CuCN)_2WS_4]$		470,435	[53]
$[PPh_4]_2[(CuCl)_2WS_4]$		435	[53]
$[Et_4N][(PPh_3)_2Ag(CuCN)WOS_3]$	925	455,426,410	[63]
$[(PPh_3)_3Ag_2WOS_3]$	935	455,436,415	[65]
$[(PPh_3)_3\{S_2P(OEt)_2\}Ag_3WOS_3]$	942	446,430,415	[77]
$[(PPh_3)_3Cu_3ClWS_4]$	513	436	[88]
$[(PPh_3)_3Cu_3ClWOS_3]$	929	436	[88]
$[PPh_4]_2[(CuCl)_3WS_4]$		460,430	[68]
$[NEt_4]_3[(\mu_2\text{-}Br)(CuBr)_3WOS_3]$	914	435	[24]

Table 2 (*continued*)

Compound	M–X_t	M–X'_{Br}	Reference
$[(AsPh_3)_3IAg_3WS_4](SAsPh)$	508	427	[42]
$[(AsPh_3)_3BrCu_3WOS_3]$	936	424	[42]
$[(PPh_3)_3ICu_3WOS_3]$	935	434	[42]
$[(Py)_5ICu_3WOS_3]$	928	431	[42]
$[NEt_4]_2[(CuNCS)_3WS_4]$		471,461,444	[70]
$[biPy_2Cl_{1.75}Cu_{3.75}WS_4]$	505	470,438	[104]
$[PPh_4]_2[(CuNCS)_4WS_4]$		433	[70]
$[NEt_4]_3[Cu_4(NCS)_5WS_4]$		442	[70]
$[(\gamma\text{-pic})_4(NCS)_2Cu_4WS_4]$		432	[19]
$[Py_4(SCN)_2Cu_4WS_4]$		430	[19]
$[(PPh_3)_4Cu_4W_2O_2S_6]$	937	438	[127]
$[(AsPh_3)_4Ag_4W_2S_8]$	511	469,434	[128]
$[(PPh_3)_4(SCMe_3)_2Cu_6W_2O_2S_6]$	940	460	[75]
$[(PPh_3)_4(SCMe_3)_2Ag_6W_2O_2S_6]$	949	425	[77]
$[(PMePh_2)_4Cu_2WSe_4]$		300,285,280	[56]
$[(PMePh_2)_4Ag_2WSe_4]$		325,315	[56]
$[(PPh_3)_3ClCu_3WSe_4]$	320	305,295	[56]

Mo(W)–Cu–S clusters are associated with the Cu atoms; those observed at −0.08 V and 0.01 V are associated with the Ag atoms.

6. Non-linear optical properties

Research on NLO materials in the last decade has been largely focused on semiconductors, conjugated polymers, discrete organic molecules [155,156], fullerenes [31,157–159] and metallophthalocyanine complexes [160]. Inorganic clusters, in this regard, have received little attention. This is unfortunate because inorganic clusters possess, in principle, the combined strength of both semiconductors and organic molecules. The advantage that inorganic clusters have over most organic molecules is that they contain many heavy atoms. The incorporation of heavy atoms introduces more sublevels into the energy hierarchy compared with organic molecules with the same number of skeleton atoms, which permits more allowed electronic transitions to take place and hence larger NLO effects. Compared with semiconductors, where few structural changes can be implemented, both the skeletal and terminal atoms of the clusters can be altered and/or removed. Both linear and non-linear optical properties can be altered and optimized separately through structural manipulations. About 20 Mo(W)–Cu(Ag)–S clusters [42] were synthesized recently to measure their NLO properties.

6.1. Butterfly-shaped clusters [27]

The NLO properties of cluster $[(PPh_3)_4Cu_2WOS_3]$ are relatively simple. It is dominated by non-linear refraction (self-focusing) as illustrated by the Z scan trace

Table 3
Chemical shift (ppm) of the NMR peaks of some Mo(W)–Cu(Ag)–S(Se) clusters

Cluster	^{95}Mo	^{183}W	^{33}S	^{77}Se	Reference
$(NH_4)_2MoS_4$	2207[b]		344[d]		[45]
$(NH_4)_2MoOS_3$	1587[b]				[45]
$(NH_4)_2MoO_2S_2$	964[b]				[45]
$[^nPr_4N][NCCu)MoS_4]$	1863[b]		445[b]		[44,150]
$[^nPr_4N][(NCAg)MoS_4]$	1921[b]		257[b]		[45,150]
$[^nPr_4N][(PhSCu)MoS_4]$	1903[b]		436[b]		[46,150]
$[Et_4N]_2[(NCCu)MoOS_3]$	1198[b]				[45]
$[Ph_4P]_2[(PhSCu)MoO_2S_2]$	611[c]				[48]
$[^nPr_4N]_2[(PhSCu)_2MoS_4]$	1700[b]				[48]
$[Ph_4P]_2[(BrCu)_2MoS_4]$	1632[c]				[48]
$[Ph_4P]_2[(ClCu)_2MoS_4]$	1618[c]				[48]
$[Ph_4P]_2[(NCCu)_2MoS_4]$	1616[c]				[45]
$[Et_4N]_2[(NCCu)_2MoS_4]\cdot H_2O$	1606[c]		139[b]		[45]
$[(PPh_3)_3Ag_2MoS_4]$	1848[a]				[151]
$[(PPh_3)_4Ag_2MoS_4]$	1863[a]				[151]
$[(PPh_3)_3Cu_2MoS_4]$	1727[a]				[151]
$[(PPh_3)_3Cu_2MoOS_3]$	1005[a]				[151]
$[^nPr_4P]_2[(ICu)_3MoS_4]$	1282[b]				[48]
$[Ph_4P]_2[(BrCu)_3MoS_4]$	1272[c]				[48]
$[Ph_4P]_2[(ClCu)_3MoS_4]$	1234[c]				[48]
$[Et_4P]_2[(Et_2NCS_2)_3Cu_3MoS_4]$	1296[c]				[130]
$[Ph_4P]_2[(BrCu)_4MoS_4]$	910[c]				[48]
$[Ph_4P]_2[(ClCu)_4MoS_4]$	886[c]				[48]
$[Et_4N]_2[(Me_2NCS_2)_3Cu_5Mo_2S_8]$	995[c]				[130]
$[Et_4N]_2[(Me_2NCS_2)_3Cu_5Mo_2S_6O_2]$	830[c]				[130]
$[Ph_4N]_2[(Et_2NCS_2)_3Cu_5Mo_2S_6O_2]$	830[c]				[130]
$[Et_4N]_2[WS_4]$		3769[c]	183[b]		[45]
$[Et_4N]_2[WO_2S_2]$		1787[e]			[45]
$[^nPr_4N]_2[(NCCu)WS_4]$		3084[c]	248[b]		[45,150]
$[^nPr_4N]_2[(NCAg)WS_4]$		3185[c]	106[b]		[45,150]
$[^nPr_4N]_2[(NCCu)_2WS_4]\cdot H_2O$		2641[c]	16[b]		[45,150]
$[Et_4N]_2[(NCCu)WOS_3]$		1994[c]			[45]
$[\{(PMe_2Ph)_2Cu\}_2WSe_4]$				1044[c]	[56]
$[\{(PMe_2Ph)_2Ag\}_2WSe_4]$				1092[c]	[56]
$[(PPh_3)_3Cu_3ClWSe_4]$				1232,1651[c]	[56]

[a] In CH_2Cl_2. [b] In CH_3CN. [c] In DMF. [d] In H_2O. [e] In D_2O.

in Fig. 16. With a 1.2×10^{-4} mol dm^{-3} solution of $[(PPh_3)_4Cu_2WOS_3]$ in acetonitrile, the effective non-linear refractive index n_2 was measured to be 8×10^{-18} m^2 W^{-1}. The effective third-order NLO susceptibility $\chi^{(3)}$ was therefore calculated to be 2×10^{-11} esu from the n_2 value (corresponding molecular hyperpolarizability $\gamma=9\times10^{-29}$ esu). Non- linear refractive indices n_2 (m^2 W^{-1}) have been reported for some of the best NLO materials such as inorganic oxides (SiO_2 (2×10^{-20}) and PN (1.3×10^{-18})), semiconductors (CdS (2.5×10^{-18}), CdSe (-7.3×10^{-19}) and GaAs

Table 4
Cyclic voltammograms of some Mo(W)–Cu(Ag)–S compounds

Compound	E_1(ox)	E_1(red)	E_2(ox)	E_2(red)	E_3(red)	Reference
$[Et_4N]_3[(\mu_2\text{-}Br)(CuBr)_3MoOS_3]$	0.50	0.42	−0.36			[25]
$[Et_4N]_3[(\mu_2\text{-}Br)(CuBr)_3WOS_3]$	0.50	0.41	−0.37			[24]
$[(AsPh_3)_3Cu_3BrWOS_3]$	0.52	0.40				[42]
$[(AsPh_3)_3Cu_3IWOS_3]$	0.56	0.40				[42]
$[(n\text{-}Bu)_4N]_2[BrCl_2Cu_3MoOS_3]$	0.51	0.40		−1.53	−1.75	[26]
$[Et_4N]_4[I_6Cu_4MoS_4]$	0.56	0.43		−0.69	−1.41	[103]
$[Et_4N]_4[I_6Cu_4WS_4]$	0.56	0.42		−0.75		[103]
$[(AsPh_3)_4Ag_4W_2S_8]$	−0.08	−0.10		−1.25	−1.75	[128]
$[(AsPh_3)_3Ag_3IWS_4](SAsPh_3)$	0.07	−0.10		−1.25	−1.75	[42]

The data were measured in CH_3CN solutions containing 0.1 mol dm^{-3} of Et_4NClO_4 as supporting electrolyte with platinum as working and auxiliary electrodes and a saturated coloured electrode (SCE) as reference electrode under a nitrogen atmosphere.

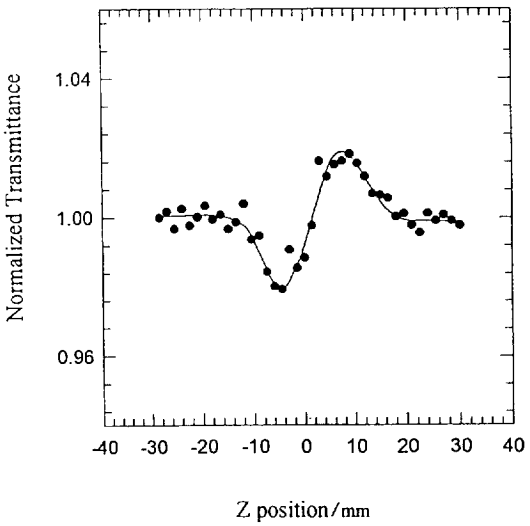

Fig. 16. The Z scan trace showing self-focusing effect of $[(PPh_3)_4Cu_2WOS_3]$.

(-1.6×10^{-17})) and organic polymers (poly-4BCMU (5×10^{-18}), DANS (8×10^{-18}) and PTS (-2×10^{-16})) at 1.06 and 1.31 μm [161–163]. Although the n_2 value of 8×10^{-18} m^2 W^{-1} was obtained with a 1.2×10^{-4} mol dm^{-3} solution of $[(PPh_3)_4Cu_2WOS_3]$, this is comparable with these best known third-order NLO materials in neat solid form. The upper limit of the concentration (1.2×10^{-4} mol dm^{-3}) of the cluster in solution is currently controlled by the low solubility of the cluster in common organic solvents. A much larger n_2 value may be expected if a much higher concentration can be achieved.

Cluster $[(PPh_3)_3Cu_2MoOS_3]$ exhibits both NLO absorption (Fig. 17(a)) and

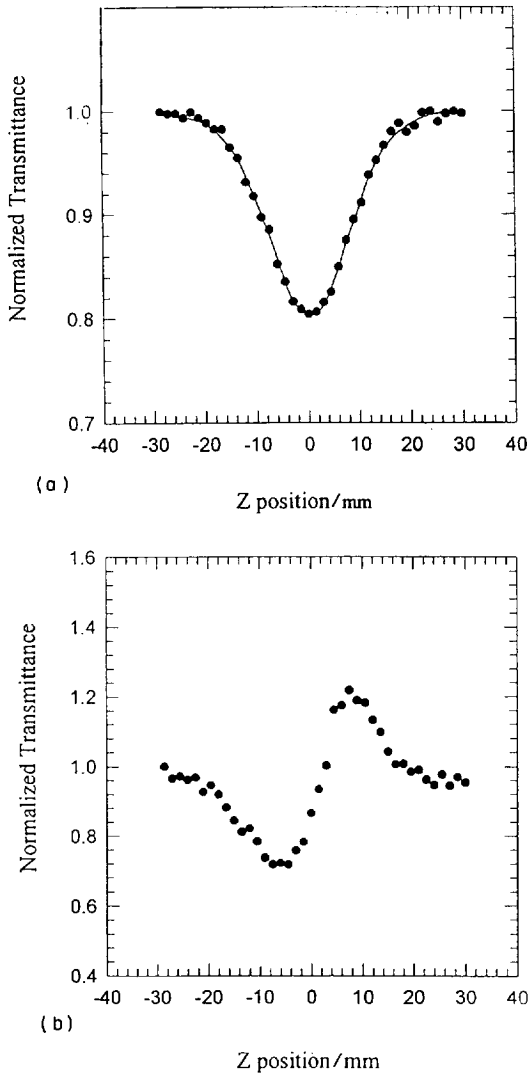

Fig. 17. (a) The NLO absorption of $[(PPh_3)_3Cu_2MoOS_3]$. (b) The NLO refraction of $[(PPh_3)_3Cu_2MoOS_3]$.

refraction (Fig. 17(b)). The effective NLO absorption coefficient α_2 and the effective refraction index n_2 were determined to be 2.6×10^{-10} m W^{-1} and 5×10^{-17} m^2 W^{-1} respectively for a 7.4×10^{-5} mol dm^{-3} solution. From the α_2 and n_2 values, the effective third-order NLO susceptibility $\chi^{(3)}$ was calculated to be 1.2×10^{-10} esu ($\gamma = 8.9 \times 10^{-28}$ esu). The $\chi^{(3)}$ values of some of the best organic polymers and semiconductors include 8.5×10^{-10} esu for PDA-PTS, 1.8×10^{-10} esu for PDA-4BCMU, 5.0×10^{-10} esu for PA, 4.8×10^{-11} esu for GaAs and 4×10^{-10} esu for Ge [164,165].

6.2. Nest-shaped clusters

Cluster $[(n\text{-}Bu)_4N]_2[BrCl_2Cu_3MoOS_3]$ exhibits interesting self-defocusing and non-linear absorptive properties [26]. The large self-defocusing effect and the strong non-linear absorption at 532 nm are clearly shown in Fig. 18(a). The combination of self-defocusing and non-linear absorption makes the cluster an interesting candidate for optical limiting applications [166–168]. The optical limiting capability utilizing only the non-linear absorption of the cluster is demonstrated in Fig. 18(b). The light energy transmitted starts to deviate from Beer's law as the light fluence

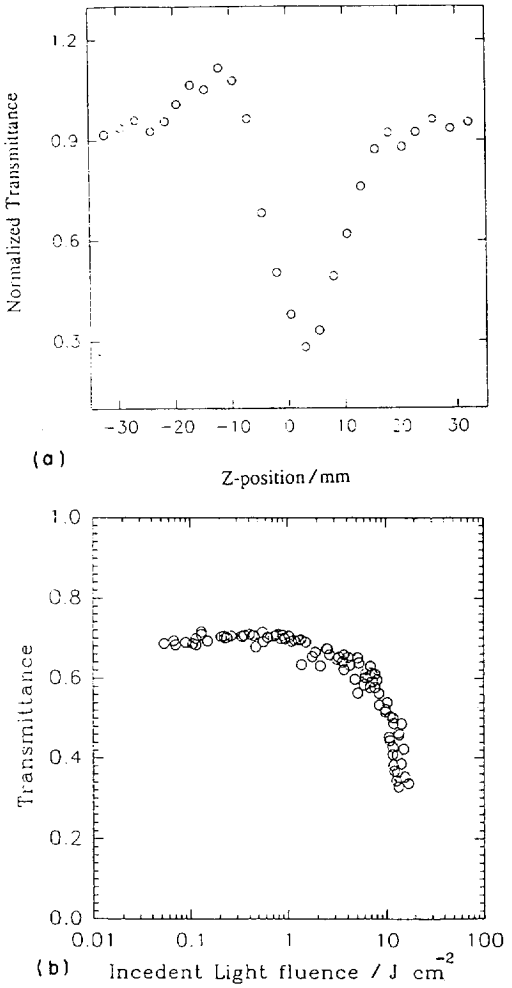

Fig. 18. (a) The NLO refraction of $[(n\text{-}Bu)_4N]_2[BrCl_2Cu_3MoOS_3]$. (b) The optical limiting capability of $[(n\text{-}Bu)_4N]_2[BrCl_2Cu_3MoOS_3]$.

reaches about 1 J cm^{-2}, and the materials become increasingly less transparent as the light fluence rises. The saturation fluence transmitted is approximately 10 J cm^{-2}.

Another nest-shaped cluster $[(n\text{-}Bu)_4N]_2[(NCS)_3Cu_3MoOS_3]$ was discovered to have a very large effective third-order hyperpolarizability ($\gamma = 4.8 \times 10^{-29}$ esu) as measured by degenerate fow-wave mixing (DFWM). It also exhibits a large optical limiting effect [28].

6.3. Half-open cubane-like clusters

The non-linear absorption component of a half-open cubane-like cluster $[Et_4N]_3[(\mu_2\text{-}Br)(CuBr)_3WOS_3]\cdot 2H_2O$ [24] was evaluated by a Z scan experiment under an open aperture configuration. The measured α_2 value is 6.0×10^{-10} m W^{-1}. The non-linear refractive component was measured by Z scan under a closed aperture configuration. The refractive index n_2 was calculated to be 1.1×10^{-16} m^2 W^{-1} in a 9.4×10^{-4} mol dm^{-3} solution. From the α_2 and n_2 values, a third-order susceptibility $\chi^{(3)}$ of 2.6×10^{-10} esu ($\gamma = 1.6 \times 10^{-28}$ esu) was obtained.

6.4. Cubane-like clusters

The optical limiting capability of the cluster $[(n\text{-}Bu)_4N]_3[L_3Ag_3BrMoS_4]$ (L≡I and Cl) [21] is depicted in Fig. 19. The limiting thresholds were measured to be 0.5 J cm^{-2} (L≡I) and 0.6 J cm^{-2} (L≡Cl), with a transmitted saturation fluence of 0.3 J cm^{-2} in both cases. These parameters are three- and twofold better than that of C_{60}, one of the most frequently cited molecular optical limiting materials.

The cluster $[(n\text{-}Bu)_4N]_3[Br_3M'BrWS_4]$ (M′≡Cu, Ag) has also demonstrated

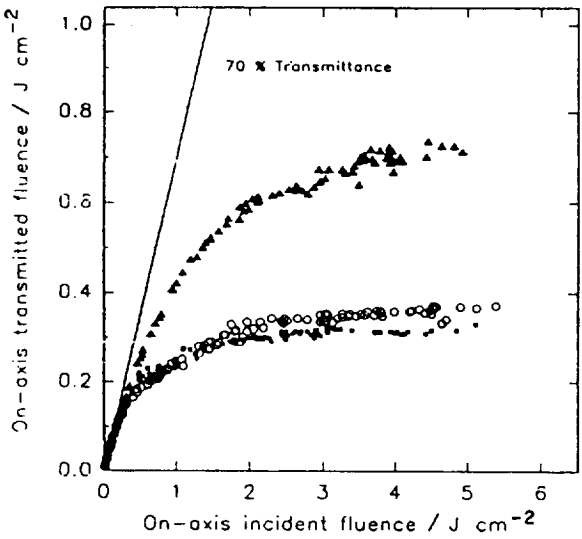

Fig. 19. The optical limiting capability of $[(n\text{-}Bu)_4N]_3[X_3Ag_3BrMoS_4]$: ■, X≡I; ○, X≡Cl; ▲, C_{60}.

excellent optical limiting capability [22]. Substitution of Cu by Ag leads to significant improvement of the limiting performance. Results of temporal profile analysis and pump-probe experiments show that the excellent optical limiting capability of the cubane-like clusters stems from their efficient excited triplet state absorption.

6.5. *Twin nest-shaped clusters*

Z scan data (Fig. 20(a)) of a twin nest-shaped cluster $[Et_4N]_4[Br_2I_4Cu_6Mo_2O_2S_6]$ [23] reveal that the compound possesses self-defocusing ability and, in addition, strong non-linear absorption at 532 nm. It is noted that the NLO properties of the

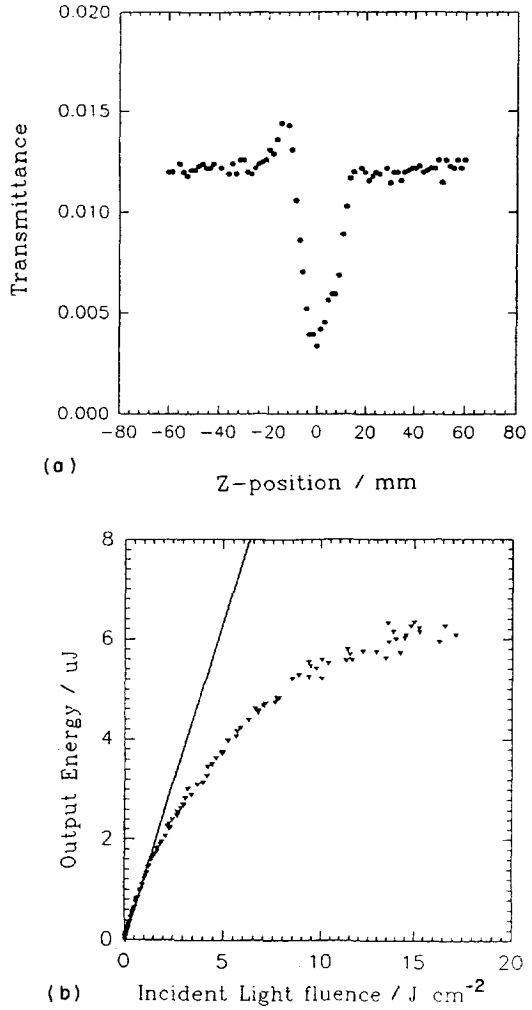

Fig. 20. (a) The self-defocusing ability of $[Et_4N]_4[Br_2I_4Cu_6Mo_2O_2S_6]$. (b) The optical limiting data of $[Et_4N]_4[Br_2I_4Cu_6Mo_2O_2S_6]$.

"dimer" (of two nest-shaped fragments) are very similar to those of the "monomers" (nest-shaped clusters). In the case of optical limiting capability (Fig. 20(b)), the light energy transmitted starts to deviate from Beer's law as the input light fluence reaches about 1.5 J cm^{-2}. The limiting threshold was measured as 2 J cm^{-2} with a transmitted saturation fluence of 8.5 J cm^{-2}.

6.6. *Hexagonal prism-shaped and supra-cage-shaped clusters*

The best optical limiting performance is achieved with the second of the two hexagonal prism-shaped clusters $[(AsPh_3)_4Ag_4W_2S_8]$ [128] and $[(PPh_3)_4Ag_4Mo_2S_8]$ [29]. The optical non-linearity of these clusters is effectively irradiance dependent, which permits them to be used for both energy limiting and power limiting. The optical limiting threshold measured for the latter cluster is one order of magnitude lower than that of C_{60}. The lower limiting threshold provides a larger safety margin for the optical device to be protected. The supra-cage-shaped cluster $[(n\text{-}Bu)_4N]_4[Cu_{12}Mo_8O_8S_{24}]$ [30] also exhibits strong third-order NLO effects ($\gamma = 5.7 \times 10^{-28}$ esu).

References

[1] B.F.C. Johnson, Transition Metal Clusters, Wiley, 1980.
[2] E.L. Muetterties, T.N. Hodin, E. Band, C.F. Brucker and W.R. Pretzer, Chem. Rev., 79 (1979) 91.
[3] F. Gaizey, Coord. Chem. Rev., 29 (1979) 195.
[4] F. Basolo, Coord. Chem. Rev., 125 (1993) 13.
[5] A. Bose and C.R. Saha, J. Mol. Catal., 49 (1989) 271.
[6] S. Bhaduri and K.R. Sharma, J. Chem. Soc., Dalton Trans., (1982) 727.
[7] G. Mclendon and A.E. Martell, Coord. Chem. Rev., 19 (1976) 1.
[8] Y. Naruta, M. Sasayama and T. Sasaki, Angew. Chem. Int. Ed. Engl., 33 (1994) 1839.
[9] D. Gatteschi, O. Kahn, J.S. Miller and F. Palacio, Magnetic Molecular Materials, Reidel, Dordrecht, 1991.
[10] R.B. King, Coord. Chem. Rev., 20 (1976) 155.
[11] O.W. Webster, J. Am. Chem. Soc., 88 (1966) 4055.
[12] F.A. Cotton and C.B. Harris, Inorg. Chem., 4 (1965) 330.
[13] J.V. Brencic and F.A. Cotton, Inorg. Chem., 8 (1969) 7.
[14] F.A. Cotton and R.A. Walton, Multiple Bond Between Metal Atoms, Wiley, New York, 1982.
[15] W.S. Ferguson, A.H. Lewis and S.J. Walson, Nature, 141 (1943) 553.
[16] X.Q. Xin, J.P. Lang, K.B. Yu, Z.Y. Zhou, M.Q. Chen, P.J. Zheng, J.H. Cai and B.S. Kang, Chin. J. Inorg. Chem., 8 (1992) 472.
[17] J.P. Lang and X.Q. Xin, J. Solid State Chem., 108 (1994) 118.
[18] A. Muller, E. Diemann, R. Jostes and H. Bogge, Angew. Chem. Int. Ed. Engl., 20 (1981) 934.
[19] S. Sarkar and S.B.S. Mishra, Coord. Chem. Rev., 59 (1984) 239.
[20] Y. Jeannin, F. Secheresse, S. Bernes and F. Robert, Inorg. Chim. Acta, 198–200 (1992) 493.
[21] S. Shi, W. Ji, S.H. Tang, J.P. Lang and X.Q. Xin, J. Am. Chem. Soc., 116 (1994) 3615.
[22] S. Shi, W. Ji, J.P. Lang and X.Q. Xin, J. Phys. Chem., 98 (1994) 3570.
[23] H.W. Hou, X.Q. Xin, J. Liu, M.Q. Chen and S. Shi, J. Chem. Soc., Dalton Trans., (1994) 3211.
[24] Z.R. Chen, H.W. Hou, X.Q. Xin, K.B. Yu and S. Shi, J. Phys. Chem., 99 (1995) 8717.
[25] S. Shi, Z.R. Chen, H.W. Hou, X.Q. Xin and K.B. Yu, Chem. Mater., 7 (1995) 1519.
[26] H.W. Hou, X.R. Ye, X.Q. Xin, J. Liu, M.Q. Chen and S. Shi, Chem. Mater., 7 (1995) 472.

[27] S. Shi, H.W. Hou and X.Q. Xin, J. Phys. Chem., 99 (1995) 4050.
[28] S. Shi, W. Ji, W. Xie, T.C. Chong, H.C. Zeng, J.P. Lang and X.Q. Xin, Mater. Chem. Phys., 39 (1995) 298.
[29] S. Shi and X.Q. Xin, J. Phys. Chem., in press.
[30] S. Shi and X.Q. Xin, J. Phys. Chem., 99 (1995) 894.
[31] L.W. Tutt and A. Kost, Nature, 356 (1992) 224.
[32] H.W. Hou, J.G. Li, J.P. Lang and X.Q. Xin, Chin. J. Inorg. Chem., 10 (1994) 218.
[33] T. Murata, M. Hidai, H. Gao, Y. Ishii, T. Wakalayashi, F. Nakano, T. Tanase, S. Yano, M. Hidai, I. Echizen, H. Nanikawa and S. Motomura, J. Am. Chem. Soc., 116 (1994) 3389.
[34] A. Muller, V.P. Fedin, E. Diemann, H. Bogge, E. Krickemeyer, D. Solter, A.M. Giuliani, R. Barbieri and P. Adler, Inorg. Chem., 33 (1994) 2243.
[35] G. Sakane, Y.G. Yao and T. Shibahara, Inorg. Chim. Acta, 216 (1994) 13.
[36] T. Shibahara, M. Yamasaki, H. Akashi and T. Katayama, Inorg. Chem., 30 (1991) 2693.
[37] R.J. Cong, Thesis, Nanjing University, China, 1987.
[38] F.J. Gao, Thesis, Nanjing University, China, 1988.
[39] K.L. Tang, H.H. Ni, X.L. Jin and Y.Q. Tang, Chin. J. Struct. Chem., 13 (1994) 300.
[40] M.F. Wang, G.C. Guo, J.S. Huang, H.H. Zhuang, Q.E. Zhang and J.X. Lu, Chin. J. Struct. Chem., 13 (1994) 221.
[41] J.G. Li, X.Q. Xin, Z.Y. Zhou and K.B. Yu, J. Chem. Soc., Chem. Commun., (1991) 250.
[42] H.W. Hou, Dissertation, Nanjing University, China, 1995.
[43] A. Muller, M. Dartmann, C. Romer, W. Clegg and G.M. Sheldrick, Angew. Chem. Int. Ed. Engl., 20 (1981) 1060.
[44] S.F. Gheller, P.A. Gazzana, A.F. Masters, R.T.C. Brownlee, M.J. O'Connor, A.G. Wedd, J.R. Rodgers and M.R. Snow, Inorg. Chim. Acta, 54 (1981) L131.
[45] S.F. Gheller, T.W. Hambley, J.R. Rodgers, R.T.C. Brownlee, M.J. O'Connor, M.R. Snow and A.G. Wedd, Inorg. Chem., 23 (1984) 2519.
[46] S.R. Actt, C.D. Garner, J.R. Nicolson and W. Clegg, J. Chem. Soc., Dalton Trans., (1983) 713.
[47] A. Muller, U. Schimanski and J. Schimanski, Inorg. Chim. Acta, 76 (1983) L245.
[48] M. Minelli, J.H. Enemark, J.R. Nicholson and C.D. Garner, Inorg. Chem., 23 (1984) 4384.
[49] C.C. Lin and Z.S. Heng, Chin. J. Struct. Chem., 8 (1989) 50.
[50] W.P. Binnic, M.J. Redman and W.J. Mallio, Inorg. Chem., 9 (1970) 1449.
[51] A. Muller and R. Menge, Z. Anorg. Allg. Chem., 393 (1972) 259.
[52] J.P. Lang, S.A. Bao, X.Q. Xin and K.B. Yu, Polyhedron, 12 (1993) 801.
[53] F. Secheresse, M. Salis, C. Potvin and J.M. Maroll, Inorg. Chim. Acta, 114 (1986) L19.
[54] C. Povin, J.M. Maroll, F. Secheresse and S. Marzak, Inorg. Chem., 26 (1987) 4370.
[55] X.L. Jin, H.H. Ni, K.L. Tang and Y.Q. Tang, Second Symposium on Metal Cluster Compounds, China, 1991, p. 7.
[56] C.C. Christak, M.A. Ansari and J.A. Ibers, Inorg. Chem., 31 (1992) 4365.
[57] X.L. Jin, H.H. Ni, K.L. Tang and Y.Q. Tang, Science in China, 11 (1986) 1136.
[58] F.G. Gao and X.Q. Xin, Chin. Gaodeng Xuexiao Huaxue Xuebao, 11 (1990) 1045.
[59] G.X. Jin, Dissertation, Nanjing University, China, 1988.
[60] J.K. Stalick, A. Siedle, A.D. Mighell and C. Hubbard, J. Am. Chem. Soc., 101 (1979) 2903.
[61] A. Muller, H. Bogge and E. Koniger-Ahlborn, Z. Naturforsch., Teil B, 34 (1979) 1698.
[62] A. Muller, H. Bogge, H.G. Tolle, R. Jostes, U. Schimanski and M. Dartmann, Angew. Chem. Int. Ed. Engl., 19 (1980) 645.
[63] N.Y. Zhu, S.W. Du, P.C. Chen, X.T. Wu and J.X. Lu, J. Coord. Chem., 26 (1992) 35.
[64] R. Cao, X.J. Lei, M.C. Hing, Z.Y. Huang and H.Q. Liu, Chin. J. Struct. Chem., 11 (1992) 34.
[65] S.W. Du, N.Y. Zhu, P.C. Chen and X.T. Wu, Polyhedron, 19 (1992) 2489.
[66] A. Beheshti and C.D. Garner, J. Sci. Islamic Repub. Iran, 1 (1990) 270.
[67] H.W. Hou, X.Q. Xin, X.Y. Huang, J.H. Cai and B.S. Kang, Chin. Chem. Lett., 6 (1995) 91.
[68] J.M. Manoli, C. Potvin and F. Secheresse, J. Chem. Soc., Chem. Commun., (1982) 1159.
[69] A. Muller, J. Schimanski and H. Bugge, Z. Anorg. Allg. Chem., 544 (1987) 107.
[70] J.M. Manoli, C. Potvin, F. Secheresse and S. Marzak, Inorg. Chim. Acta, 150 (1988) 257.
[71] J.N. Liu, X.J. Lei, B.S. Kang, Z.Y. Huang and M.C. Hong, Chin. J. Struct. Chem., 10 (1991) 196.

[72] X.J. Lei, X.T. Liu and H.Q. Liu, Chin. J. Struct. Chem., 7 (1988) 99.
[73] Z.Y. Huang, X.J. Lei, J.N. Liu, B.S. Kang, Q. Liu, M.C. Hong and H.Q. Liu, Inorg. Chim. Acta, 165 (1990) 25.
[74] J.G. Li, Dissertation, Nanjing University, China, 1990.
[75] S.W. Du, N.Y. Zhu, P.C. Chen and X.T. Wu, Angew. Chem. Int. Ed. Engl., 8 (1992) 1085.
[76] W. Clegg, A. Beheshti and C.D. Garner, Acta Crystallogr., Sect. C, 44 (1988) 170.
[77] S.W. Du and X.T. Wu, J. Coord. Chem., 30 (1993) 183.
[78] H.W. Hou, X.Q. Xin, S.F. Lu, X.Y. Huang and Q.J. Wu, J. Coord. Chem., in press.
[79] J.P. Lang, H.Z. Zhu, X.Q. Xin, M.Q. Chen, K. Liu and P.J. Zheng, Chin. J. Chem., 11 (1993) 21.
[80] J.P. Lang, S.A. Bao, H.Z. Zhu, X.Q. Xin and K.B. Yu, Chin. J. Chem., 11 (1993) 126.
[81] J.P. Lang, H.Z. Zhu, X.Q. Xin, K.B. Yu and Z.Y. Zhu, Chin. J. Struct. Chem., 11 (1992) 27.
[82] J.H. Cai, L.H. Weng, B.S. Kang, J.P. Lang, H.Z. Zhu and X.Q. Xin, Chin. J. Struct. Chem., 12 (1993) 22.
[83] J.P. Lang, Fourth Symposium on Inorganic Chemistry, China, 1992, p. 191.
[84] J.P. Lang, S.A. Bao, H.Z. Zhu, X.Q. Xin, J.H. Cai and B.S. Kang, Chin. J. Chem., 11 (1993) 302.
[85] J.H. Cai, L.H. Weng, B.S. Kang, J.P. Lang and X.Q. Xin, Seventh Symposium on Metal-Organic Chemistry, China, 1993, p. 194.
[86] J.P. Lang, Dissertation, Nanjing University, China, 1993.
[87] H.W. Hou, Y. Liu, X.Q. Xin, S.F. Lu and Q.J. Wu, Syn. React. Inorg. Metal-org. Chem., in press.
[88] A. Muller, H. Bogge and U. Schimanski, Inorg. Chim. Acta, 69 (1983) 5.
[89] X.T. Wu, J.H. Wu, N.Y. Zhu and J.X. Lu, Second Symposium on Metal Cluster Compounds, China, 1991, p. 56.
[90] A. Muller, Monatsh. Chem., 120 (1989) 367.
[91] S.X. Liu, J.L. Huang, F. Gao, H.Z. Zhu and X.Q. Xin, Chin. Gaodeng Xuexiao Huaxue Xuebao, 11 (1990) 669.
[92] J.H. Wu, N.Y. Zhu, S.W. Du, X.T. Wu and J.X. Lu, Polyhedron, 11 (1992) 1201.
[93] C.C. Lin, Z.S. Zheng and S.X. Liu, Chin. J. Struct. Chem., 10 (1991) 209.
[94] B.C. Shi, F.J. Gao, E.Y. Shao, G.C. Wei and Z.S. Jin, Chin. J. Struct. Chem., 11 (1992) 235.
[95] X.T. Wu, Y.F. Zheng, S.W. Du and N.Y. Zhu, Trans. Met. Chem., 14 (1989) 157.
[96] W. Clegg, C.D. Scattergood and C.D. Garner, Acta Crystallogr., Sect. C, 43 (1987) 786.
[97] F. Secheresse, S. Bernes, F. Robert and Y. Jeannin, J. Chem. Soc., Dalton Trans., (1991) 2875.
[98] J.R. Nicholson, A.C. Flood, C.D. Garner and W. Clegg, J. Chem. Soc., Chem. Commun., (1983) 1179.
[99] J.M. Manoli, C. Potvin, F. Secheresse and S. Marnnin, J. Chem. Soc., Chem. Commun., (1986) 1557.
[100] Y. Yang, Q.T. Liu, L.G. Huang and D.X. Wu, Second China–Japan Symposium on Metal Cluster Compounds, China, 1993, p. 45.
[101] A. Muller, E. Krickmeyer, H. Bogge and M. Penk, Chimica, 43 (1989) 319.
[102] M.T. Pope, J.P. Lang, X.Q. Xin and K.B. Yu, Chin. J. Chem., 13 (1995) 40.
[103] J.P. Lang, W.Y. Zhou, X.Q. Xin and K.B. Yu, J. Coord. Chem., 30 (1993) 173.
[104] F. Secheresse, F. Robert, S. Marzak, J.M. Manoli and C. Potvin, Inorg. Chim. Acta, 182 (1991) 221.
[105] F. Secheresse, J.M. Manoli, C. Potvin and S. Marzak, J. Chem. Soc., Dalton Trans., (1988) 3050.
[106] J.P. Lang, W.Y. Zhou, X.Q. Xin, J.H. Cai, B.S. Kang and K.B. Yu, Polyhedron, 12 (1993) 1647.
[107] F.K. Zheng and X.F. Yu, Chin. J. Struct. Chem., 13 (1994) 397.
[108] S. Bernes, F. Secheresse and Y. Jeannin, Inorg. Chim. Acta, 191 (1992) 11.
[109] C.D. Scattergood, P.G. Bonney, J.M. Slater, C.D. Garner and W.G. Clagg, J. Chem. Soc., Chem. Commun., (1987) 1749.
[110] H.W. Hou, X.Q. Xin, J. Liu and M.Q. Chen, Acta Crystallogr., submitted for publication.
[111] J.P. Lang, X.Q. Xin and K.B. Yu, J. Coord. Chem., 33 (1994) 99.
[112] A. Muller, Inorg. Chim. Acta, 65 (1982) L41.
[113] N.Y. Zhu, X.T. Wu and J.X. Lu, J. Chem. Soc., Chem. Commun., (1991) 235.
[114] N.Y. Zhu, Y.F. Zheng and X.T. Wu, Polyhedron, 10 (1991) 2743.
[115] N.Y. Zhu, Y.F. Zheng and X.T. Wu, J. Chem. Soc., Chem. Commun., (1990) 780.
[116] N.Y. Zhu, R.C. Wu and X.T. Wu, Acta Crystallogr., Sect. C, 47 (1991) 1537.
[117] R.M. Yu, S.F. Lu and J.Q. Huang, Second Symposium on Coordination Chemistry, China, 1993, p. II-6.

[118] B. Henri, G. Roland, W. Joachim and N. Bernd, J. Organomet. Chem., 393 (1990) 119.
[119] J.H. Wu, N.Y. Zhou, S.W. Du, X.T. Wu and J.X. Lu, Inorg. Chim. Acta, 185 (1991) 181.
[120] Y. Yu, Q.T. Liu and D.X. Wu, Inorg. Chim. Acta, in press.
[121] Y. Yang, Q.T. Liu, B.S. Kang and J.X. Lu, Science in China, 24 (1994) 914.
[122] C.C. Lin and Z.X. Huang, Chin. J. Struct. Chem., 9 (1990) 58.
[123] X.L. Jin, H.H. Ni, K.L. Tang and Y.Q. Tang, Chin. Gaodeng Xuexiao Huaxue Xuebao, 6 (1992) 724.
[124] A. Muller, H. Bogge, E. Koniger-Ahlborn and W. Hellmann, Inorg. Chem., 18 (1979) 2301.
[125] A. Muller, H. Bogge and E. Koniger-Ahlborn, J. Chem. Soc., Chem. Commun., (1987) 739.
[126] R. Cao, X.J. Lei, H.Q. Liu and B.S. Kang, Chin. J. Chem., in press.
[127] A. Muller, H. Bogge and T. Hwang, Inorg. Chim. Acta, 39 (1980) 73.
[128] G. Sakane, T. Shibahara, H.W. Hou, X.Q. Xin, H.C. Zeng and S. Shi, Inorg. Chem., accepted for publication.
[129] R. Doherty, C.R. Hubbard, A.D. Mighell, A.R. Siedle and J. Stewart, Inorg. Chem., 18 (1979) 2991.
[130] H.Q. Liu, R. Cao, X.J. Lei, D.W. Wu, G.W. Wei, Z.Y. Huang, M.C. Hong and B.S. Kang, J. Chem. Soc., Dalton Trans., (1990) 1023.
[131] X.J. Lei, Z.Y. Huang, Q.T. Liu, M.C. Hong and H.Q. Liu, Inorg. Chem., 28 (1989) 4302.
[132] S.W. Du, N.Y. Zhu, P.C. Chen and X.T. Wu, Polyhedron, 19 (1992) 2495.
[133] X.T. Wu, Y.F. Zheng, N.Y. Zhu and J.X. Lu, Chin. J. Struct. Chem., 7 (1988) 137.
[134] X.T. Wu, S.F. Lu, Y. Zu, Q.J. Wu and J.X. Lu, Inorg. Chim. Acta, 133 (1987) 39.
[135] H.Q. Zhen, Y.F. Zheng, X.T. Wu and J.X. Lu, Chin. J. Struct. Chem., 7 (1988) 157.
[136] S.F. Lu, H.B. Chen, J.Q. Huang, Q.L. Sun, J. Li and J.X. Lu, Second China–Japan Symposium on Metal Cluster Compounds, China, 1993, p. 74.
[137] T. Shibahara, H. Kashi and H. Kuroya, J. Am. Chem. Soc., 110 (1988) 3313.
[138] X.T. Wu, B. Wang, Y.F. Zhang and J.X. Lu, Chin. J. Struct. Chem., 7 (1988) 47.
[139] A. Muller, E. Diemann, F. Neumann and R. Menge, Chem. Phys. Lett., 16 (1972) 521.
[140] E. Diemann and A. Muller, Spectrochim. Acta, Part A, 26 (1970) 215.
[141] A. Muller and E. Diemann, J. Chem. Phys., 61 (1974) 5469.
[142] A. Muller and E. Diemann, Chem. Phys. Lett., 9 (1971) 369.
[143] M.R. Udupa, J. Indian Chem. Soc., 53 (1976) 340.
[144] G.M. Clark and W.P. Doyle, J. Inorg. Nucl. Chem., 28 (1966) 381.
[145] J. Bernholc and E.I. Stiefel, Inorg. Chem., 24 (1985) 1323.
[146] D.E. Onopko and S.A. Titov, Opt. Spektrosk., 47 (1979) 327.
[147] B.D. El-Issa, A.A. Ali and H. Zanati, Inorg. Chem., 28 (1989) 3297.
[148] A. Muller, N. Weinstock and H. Schulze, Spectrochim. Acta, Part A, 28 (1972) 1075.
[149] Gmelin Handbook of Inorganic and Organometallic Chemistry, Mo Suppl., Vol. B7, 1992, p. 279.
[150] M. Kong, R.T.C. Brownlee and A.G. Wedd, Inorg. Chem., 31 (1991) 2282.
[151] J.M. Charnock, S. Bristow, J.R. Nicholson and C.D. Garner, J. Chem. Soc., Dalton Trans., (1987) 303.
[152] A. Muller, R. Jostes, V. Fleming and R. Potthast, Inorg. Chim. Acta, 44 (1980) L33.
[153] K.P. Callahan and P.A. Iliero, J. Chem. Soc., Chem. Commun., (1979) 13.
[154] K.P. Callahan and P.A. Iliero, Inorg. Chem., 19 (1980) 2619.
[155] D.S. Chemla and J. Zyss, Nonlinear Optical Properties of Organic Molecules and Crystals, Academic, Orlando, 1987.
[156] H. Huang, Optical Nonlinearities and Instabilities in Semiconductors, Academic, Boston, 1988.
[157] F. Henari, J. Callaghan, H. Stiel, W. Blau and D.J. Cardin, Chem. Phys. Lett., 199 (1992) 144.
[158] A. Kost, L. Tutt, M.B. Klein, T.K. Dougherty and W.E. Elias, Opt. Lett., 18 (1993) 334.
[159] D.G. Mclean, R.L. Sutherland, M.C. Brant, D.M. Brandelik, P.A. Fleitz and T. Pottenger, Opt. Lett., 18 (1993) 858.
[160] T.H. Wei, D.J. Hagan, M.J. Sence, E.W. Van Stryland, J.W. Perry and D.R. Coulter, Appl. Phys. B, 54 (1992) 46.
[161] J.L. Bredas, C. Adant, P. Tackx and A. Persoons, Chem. Rev., 94 (1994) 243.
[162] R. Adair, L.L. Chase and S.A. Payne, Phys. Rev. B, 39 (1989) 3337.
[163] M. Sheik-Bahae, D.C. Hutchings, D.J. Hagan and E.W. Van Stryland, IEEE J. Quantum Electron., 27 (1991) 1296.

[164] H. Nakanishi, Nonlinear Optics, 1 (1991) 223.
[165] T. Kobayashi, IEICE Trans. Fundamental, E75-A (1992) 38.
[166] M.J. Soileau, W.E. Williams and E.W. Van Stryland, IEEE J. Quantum Electron., 19 (1983) 731.
[167] E.W. Van Stryland, H. Vanherzeele, M.A. Woodall, M.J. Soileau, A.L. Smirl, S. Guha and T.F. Boggen, Opt. Eng., 24 (1985) 613.
[168] M. Sheik-Bahae, A.A. Said, D.J. Hagan, M.J. Soilean and E.W. Van Stryland, Opt. Eng., 30 (1991) 1228.